

# Internal inertia-gravity waves in the ocean

Thomas Peacock (and many, many others)

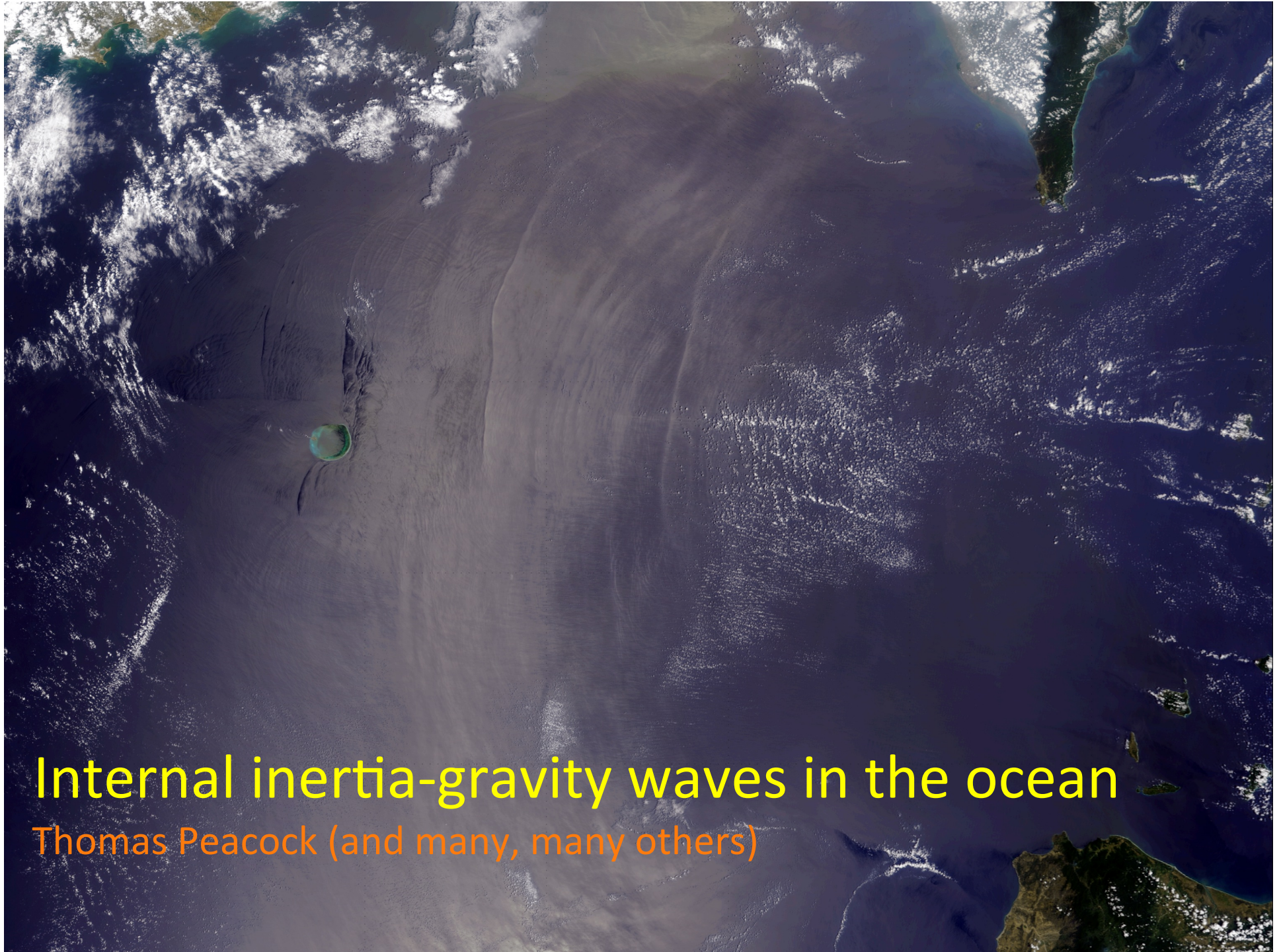


# Turbulence: The only tool you need

Thomas Peacock







# Internal inertia-gravity waves in the ocean

Thomas Peacock (and many, many others)



# Motivation

- The interior of the ocean is no quieter than the upper free surface.
- This is readily discovered by making measurements and is manifest as surface expressions of interior motion and interior oscillations of temperature and salinity.

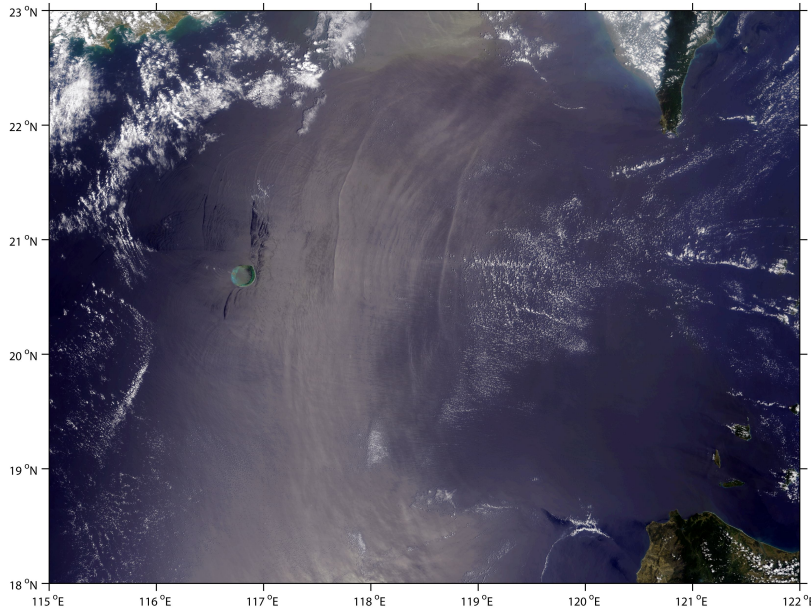


(Image: Global Ocean Associates)

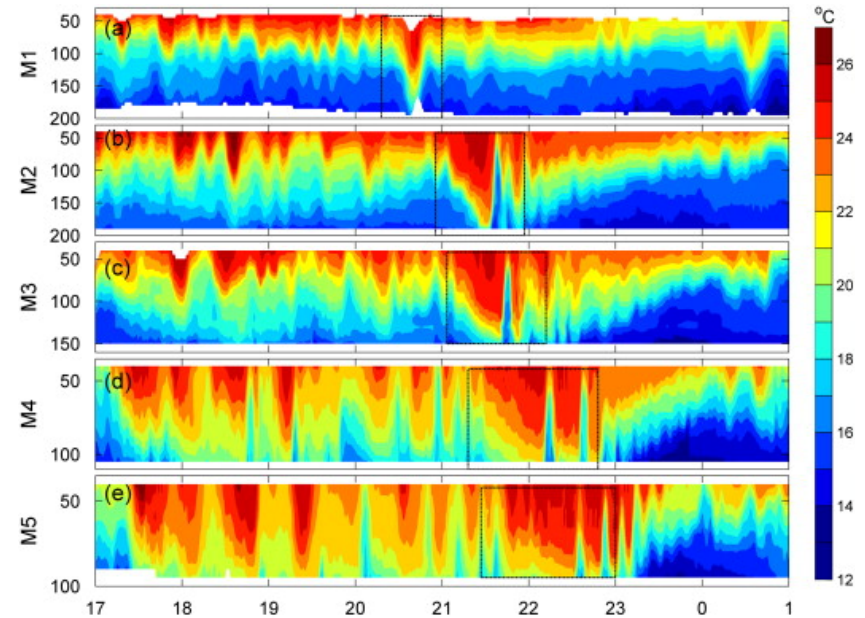


(Image: Fu et al. 2012)



# Motivation

---

- Why do we care about internal gravity waves in the ocean?

## 1. Mixing





# Motivation

---

- Why do we care about internal gravity waves in the ocean?

## 1. Mixing



## 2. Biology





# Motivation

---

- Why do we care about internal gravity waves in the ocean?

## 1. Mixing



## 2. Biology



## 3. Ocean Engineering





# Motivation

---

- Why do we care about internal gravity waves in the ocean?

## 1. Mixing



## 2. Biology



## 3. Ocean Engineering



## 4. Acoustics



# History

---

- As early as 1762 Benjamin Franklin had noticed that waves can be formed at the interface between oil and water in a glass tumbler.



“At supper, looking on the lamp, I remarked that tho’ the surface of the oil was perfectly tranquil, and duly preserved its position and distance with regard to the brim of the glass, the water under the oil was in great commotion, rising and falling in irregular waves, which continued during the whole evening. The lamp was kept burning as a watch light all night, till the oil was spent, and the water only remain’d. In the morning I observed, that though the motion of the ship continued the same, the water was now quiet, and its surface as tranquil as that of the oil had been the evening before. At night again, when oil was put upon it, the water resum’d its irregular motions, rising in high waves almost to the surface of the oil, but without disturbing the smooth level of that surface.”

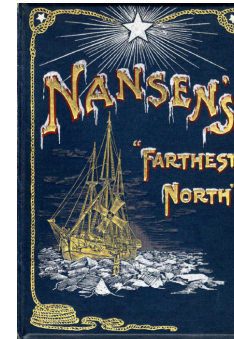
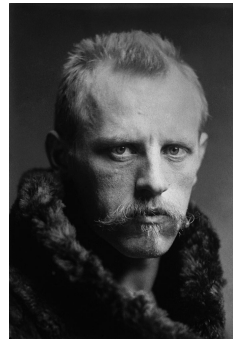
*(Oil & Water, Benjamin Franklin 1762)*



# History

---

- An early report of internal gravity waves was by Fridtjof Nansen (1897)



“We approached the ice to make fast to it, but the *Fram* had got into dead-water, and made hardly any way, in spite of the engine going full pressure. It was such slow work that I thought I would row ahead to shoot seal. In the meantime the *Fram* advanced slowly to the edge of the ice with her engines still going at full speed.”

“The ice that covered the sound north of Teimur Island was in a state of dissolution and apparently melting very rapidly, and this was probably the main cause of the sea in the sound being covered with a fresh-water layer. I only say in the journal that the water at the surface was almost fresh (drinking water), whereas through the bottom-cock of the engine room we got perfectly salt water. I suppose that the bottom-cock at that time was about 4m or more below the surface of the water, and accordingly the *Fram* struck the salt water.”

- Dead water is a consequence of internal wave dynamics.

[video](#)

(Movie: Mercier & Dauxois)

# History

---

- Ekman (1904) explained the true nature of dead water.
- Petterson (1909) reported on measurements of temperature fluctuations in a fjord, although he was preceded by lake measurements in Lac de Longemer in the Vosges region of France (Thoulet 1894) and Loch Ness in Scotland (Watson 1903).
- Attention given to internal waves waned in 1920's-1940's, their presence being regarded as noise – “One man's noise is another man's signal” (Walter Munk).
- Interest rekindled in 1960's-70's by the role of internal waves in diapycnal heat transfer (Munk 1966)
- The “St. Andrew's Cross” laboratory experiments of Mowbray & Rarity (1967) were very visual.
- Interest in internal waves grew due to their impact on deep sea operations (Osborne et al 1978) and submarine operations during the Cold War.
- Interest resurged due to results from satellite altimetry data revealing the strong generation of internal tides by deep ocean ridges (Ray & Mitchum 1996) and reconsideration of their potential significance to ocean mixing (Munk & Wunsch 1998).



*(Partial source: The Turbulent Ocean, Thorpe)*



# Basic Equations

---



*(Image: Drew, SIO)*

# Basic equations

- The starting point for modeling oceanic internal gravity waves is the linearized, Boussinesq equations for a fluid on a rotating earth within the traditional  $f$ -plane approximation:

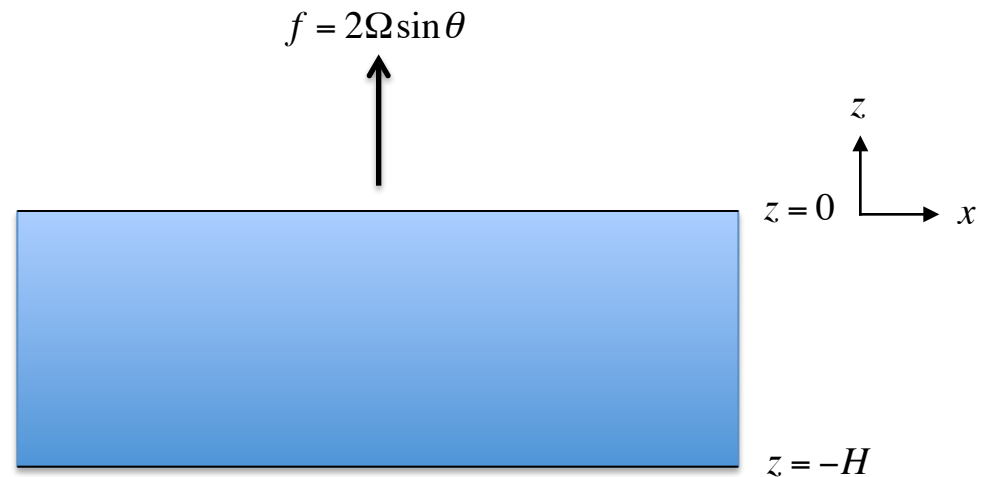
*Incompressibility:* 
$$\frac{\partial u}{\partial x} + \frac{\partial v}{\partial y} + \frac{\partial w}{\partial z} = 0$$

*Momentum:* 
$$\frac{\partial u}{\partial t} - fv = -\frac{1}{\rho_*} \frac{\partial p}{\partial x}$$

$$\frac{\partial v}{\partial t} + fu = -\frac{1}{\rho_*} \frac{\partial p}{\partial y}$$

$$\frac{\partial w}{\partial t} = -\frac{1}{\rho_*} \frac{\partial p}{\partial z} - \frac{\rho}{\rho_*} g$$

*Continuity:* 
$$\frac{\partial \rho}{\partial t} + w \frac{\partial \rho_0}{\partial z} = 0$$



- These can be reduced to the linear internal wave equation:

$$\frac{\partial^2}{\partial t^2} [\nabla^2 w] + f^2 \frac{\partial^2 w}{\partial z^2} + N^2(z) \nabla_h^2 w = 0 \quad \text{where} \quad N^2(z) = -\frac{g}{\rho_*} \frac{d\rho_0}{dz}.$$



# Vertical modes

---

- Since the ocean has both a surface and a bottom, a convenient and reasonable approximation is to treat the ocean surface as a rigid lid, so that the boundary conditions are:

$$w(0) = w(-H) = 0.$$

- Assuming waves that are sinusoidal in time, i.e.  $w \sim e^{-i\omega t}$ , and two-dimensional, i.e.  $\partial/\partial y = 0$ , the internal wave equation reduces to:

$$\left(N^2(z) - \omega^2\right) \frac{\partial^2 w}{\partial x^2} - \left(\omega^2 - f^2\right) \frac{\partial^2 w}{\partial z^2} = 0.$$

- This can be solved using the method of vertical modes:

$$w = W(z)e^{ikx} \rightarrow \frac{d^2 W(z)}{dz^2} + k^2 \frac{N^2(z) - \omega^2}{\omega^2 - f^2} W(z) = 0.$$

- Together with the boundary conditions, this constitutes a Sturm-Liouville problem and its solution is formed by a set of eigenvalues,  $k_n$ , and eigenfunctions,  $W_n$ .



# Vertical modes

---

- Within the linear approximation, the other physical variables can all be expressed in terms of the vertical velocity. For example:

$$U = \frac{i}{k} \frac{dW}{dz}; \quad V = \frac{f}{\omega k} \frac{dW}{dz}.$$

- The vertical modes satisfy an orthogonality relation:

$$\int_{-H}^0 \left( \frac{N^2(z) - \omega^2}{\omega^2 - f^2} \right) W_m W_n = 0 \quad \text{for } m \neq n.$$

- The general solution of the wave equation consists of a superposition of modes:

$$w = \sum_n w_n W_n(z) e^{i(k_n x - \omega t)}$$

where  $w_n$  is the complex amplitude of mode  $n$  (i.e. how much and what phase).

# Constant stratification

- For a constant stratification, the modes can be determined analytically.
- The governing equation for the mode shapes becomes:

$$\frac{d^2W}{dz^2} + m^2W = 0 \quad \text{where} \quad m^2 = k^2 \frac{N^2 - \omega^2}{\omega^2 - f^2}.$$

- Solving using the boundary conditions at the ocean surface and floor gives:

$$W(z) = W_n \sin m_n z, \quad \text{with} \quad m_n = \pm \frac{n\pi}{H} \quad \text{for} \quad n = 1, 2, 3, \dots$$

- The vertical structure is independent of forcing frequency.

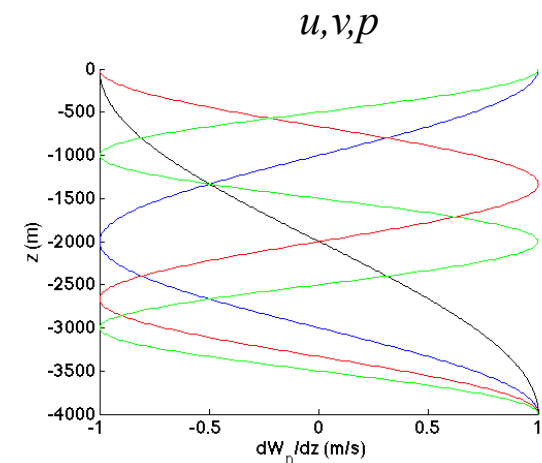
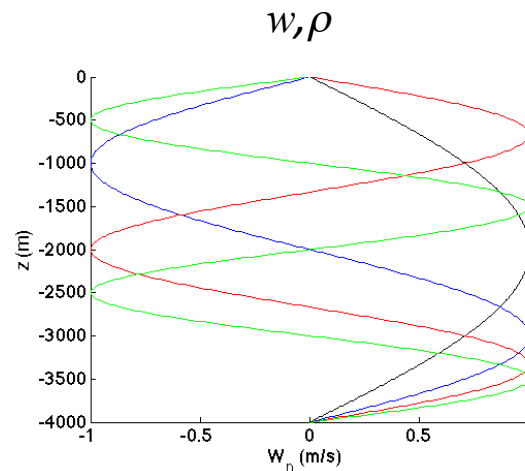
*Mode shapes:*

$H = 4000\text{m},$

$N = 0.005\text{rad/s}$

$\omega = 0.0001405\text{rad/s}$

$f = 0.0001046\text{rad/s}$

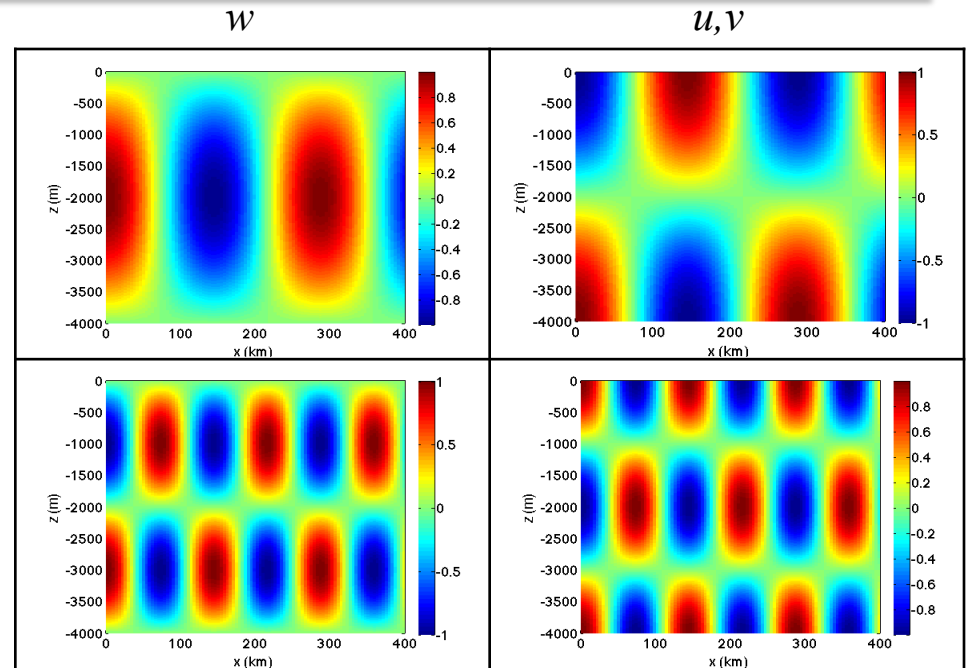




# Wave fields

- Wave fields for the different vertical modes are manifest as follows:
- Horizontal wave lengths are on the order of 50-100km for modes 1 and 2, and phase speeds are on the order of 1m/s.

Mode 1:



Mode 2:

- The dispersion relation  $k_n = \pm \frac{n\pi}{H} \left( \frac{\omega^2 - f^2}{N^2 - \omega^2} \right)^{1/2}$  has propagating solutions for:  $f < \omega < N$  (and  $N < \omega < f!$ )
- Rewriting the dispersion relation,  $\omega^2 = \frac{N^2 k^2 + f^2 m^2}{k^2 + m^2}$ , the phase and group velocities of the modes are:

$$c_p = \frac{\omega}{k} = \pm \left( \frac{H\omega}{n\pi} \right) \left( \frac{N^2 - \omega^2}{\omega^2 - f^2} \right)^{1/2}$$

$$c_g = \frac{\partial \omega}{\partial k} = \pm \left( \frac{H}{n\pi} \right) \frac{(\omega^2 - f^2)^{1/2} (N^2 - \omega^2)^{3/2}}{\omega(N^2 - f^2)}$$



Higher modes propagate more slowly.

# Laboratory experiments

---

- A novel internal wave generator developed by Gostiaux et al. (2007) enables the direct excitation of vertical modes in laboratory experiments.
- Laboratory experiment for  $H = 0.416$  m,  $N = 0.85$  rad/s,  $\omega = 0.6$  rad/s (Mercier et al. 2010).

video

*(Movie: Mathur)*

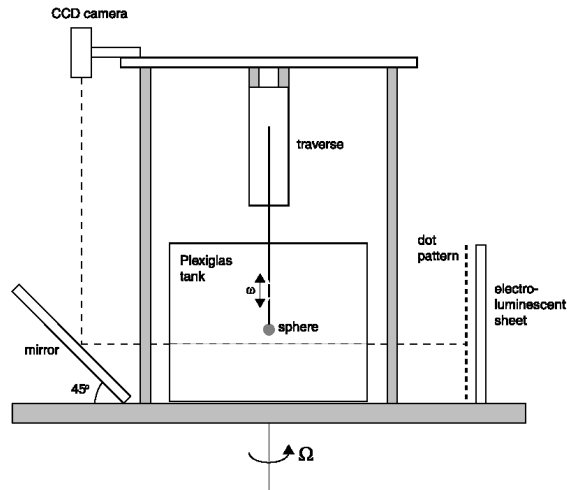
- Horizontal wavelength of mode 2 is 0.416 m with a phase speed of 0.040 m/s.



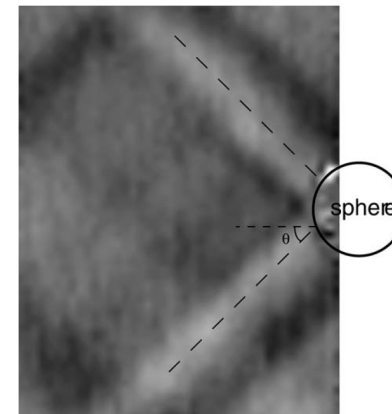
# Laboratory experiments

- Using an oscillating sphere arrangement, the lower and upper bounds of the frequency of propagation can be observed (Peacock & Weidman, 2005).

Experimental arrangement

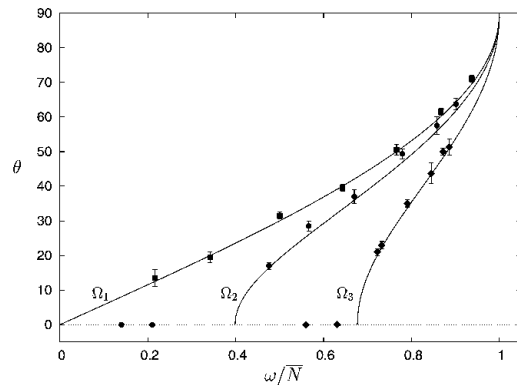


Synthetic schlieren visualization



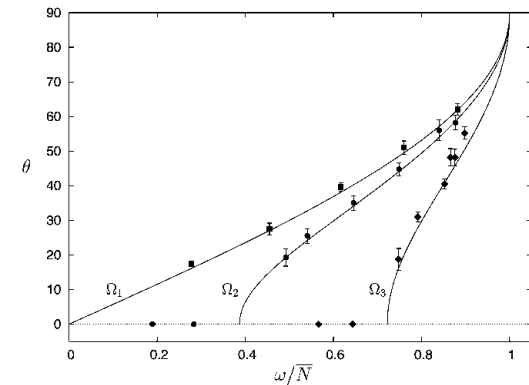
Results:

$N = 1.06 \text{ rad/s}$ ,  
 $\Omega_1 = 0.0 \text{ rad/s}$   
 $\Omega_2 = 0.205 \text{ rad/s}$   
 $\Omega_3 = 0.383 \text{ rad/s}$



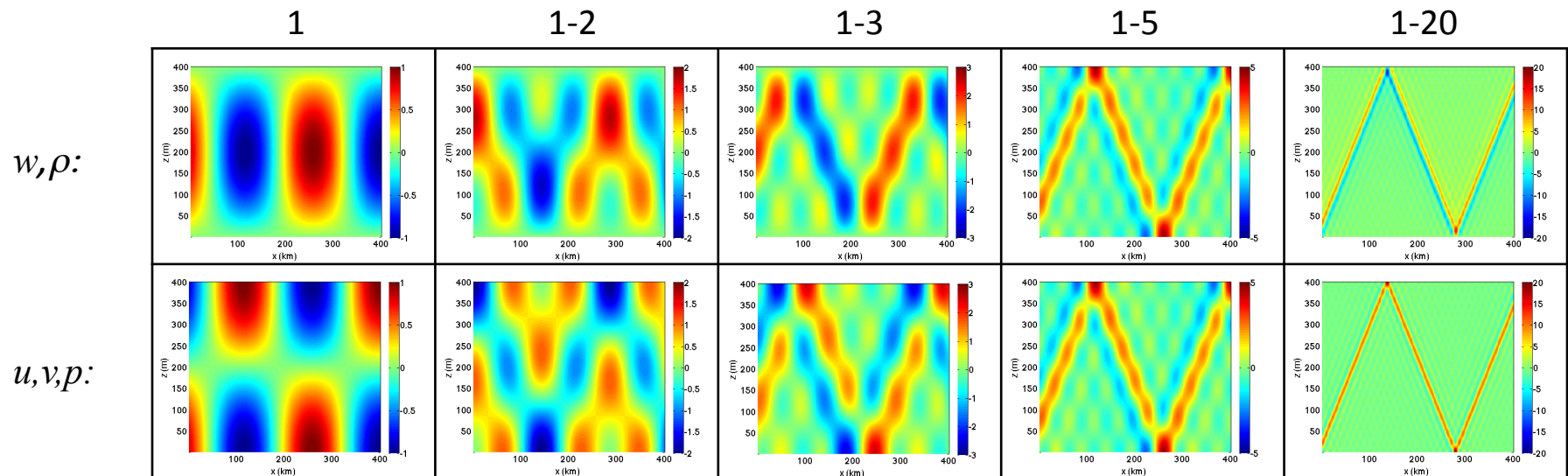
Results:

$N = 1.43 \text{ rad/s}$ ,  
 $\Omega_1 = 0.0 \text{ rad/s}$   
 $\Omega_2 = 0.285 \text{ rad/s}$   
 $\Omega_3 = 0.484 \text{ rad/s}$



# Superposition

- The wavelength of the first mode is twice that of the second, three times that of the third, etc... (i.e.  $k_1=k_2/2=k_3/3 \dots$ )  $\longrightarrow$  A superposition of modes is horizontally periodic.
- What happens if we start adding modes (we have freedom to choose amplitude and phase)?



- As a result of the superposition of modes, spatially coherent internal wave beams become evident.

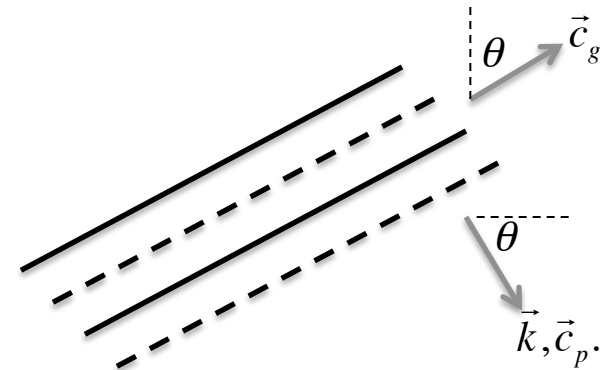
# Wave beams

- The appearance and nature of coherent internal wave beams in this idealized ocean is a consequence of:

1. Individual modes being a superposition of upward and downward plane waves, i.e.  $\cos mz = \frac{1}{2}(e^{imz} + e^{-imz})$ .

2. The ratio of vertical and horizontal wavenumbers is independent of mode, i.e.  $\frac{m_n}{k_n} = \pm \left( \frac{N^2 - \omega^2}{\omega^2 - f^2} \right)^{1/2}$ .

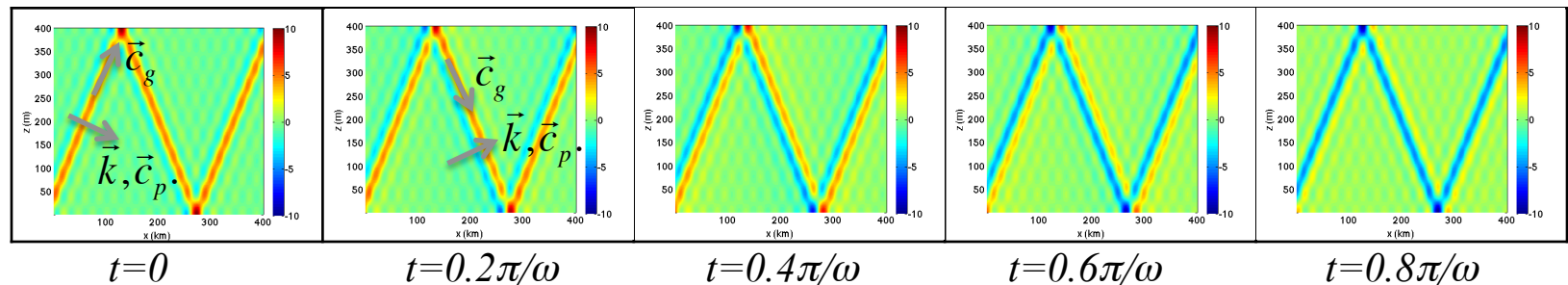
3. The properties of the underlying plane waves, i.e.  $\vec{c}_g \perp \vec{k}, \vec{c}_p$ .



$$\omega^2 = N^2 \cos^2 \theta + f^2 \sin^2 \theta$$

- Particle motion is along beams (and into the page); phase propagates through beams.

$u, v, p$ :





# Energy flux

- An important consideration is the energy flux of the vertical modes.
- Multiply linear momentum equations as follows:

$$\begin{aligned}
 & \left[ \frac{\partial u}{\partial t} - fv = -\frac{1}{\rho_*} \frac{\partial p}{\partial x} \right] \times u \\
 & \left[ \frac{\partial v}{\partial t} + fu = -\frac{1}{\rho_*} \frac{\partial p}{\partial y} \right] \times v \\
 & \left[ \frac{\partial w}{\partial t} = -\frac{1}{\rho_*} \frac{\partial p}{\partial z} - \frac{\rho}{\rho_*} g \right] \times w \\
 & \left[ \frac{\partial \rho}{\partial t} + w \frac{d\rho_0}{dz} = 0 \right] \times \left( \frac{g^2 \rho}{\rho_* N^2} \right)
 \end{aligned}
 \xrightarrow{\text{add equations}}
 \underbrace{\frac{1}{2} \rho_* \frac{\partial}{\partial t} [u^2 + v^2 + w^2]}_{KE}
 + \underbrace{\frac{1}{2} \frac{\partial}{\partial t} \left[ \frac{g \rho^2}{\rho_* N^2} \right]}_{PE}
 + \underbrace{\nabla \cdot (\vec{u} p)}_{\text{Energy Flux}} = 0$$

- Calculate time averaged, depth integrated energy flux for mode  $n$ :

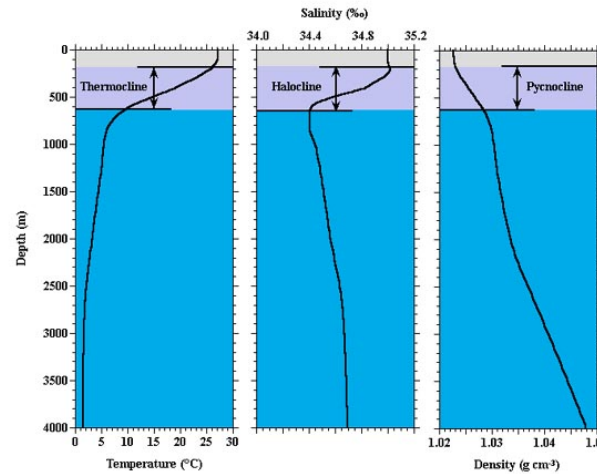
$$\int_{-H}^0 \langle up \rangle dz = \int_{-H}^0 \left\langle u_n^2 \frac{\rho_* (\omega^2 - f^2)}{\omega k_n} U_n^2(z) \cos^2(k_n x - \omega t) \right\rangle dz = \frac{u_n^2 \rho_* (\omega^2 - f^2)}{k_n 2\omega}$$

- For constant stratification, this becomes:

$$\int_{-H}^0 \langle up \rangle dz = \frac{u_n^2 \rho_* H}{n 2\pi\omega} (\omega^2 - f^2)^{1/2} (N^2 - \omega^2)^{1/2} \longrightarrow \text{For a given amplitude, higher modes carry less energy.}$$

# Nonuniform stratifications

- Of course, the density stratification of the ocean is not constant but typically varies significantly within the upper few hundred meters.



- Due to combinations of water from different origins, and also physical processes such as double diffusion, for example, the stratifications can be complex.

## Western Arctic Ocean

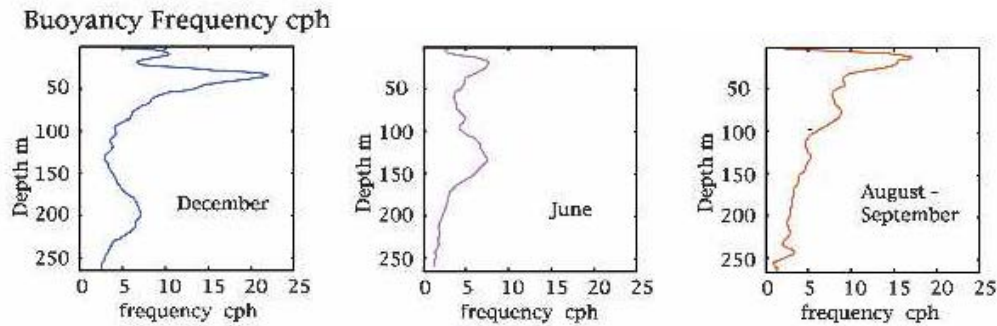


(Image: Pinkel 2005)

## Canada Basin

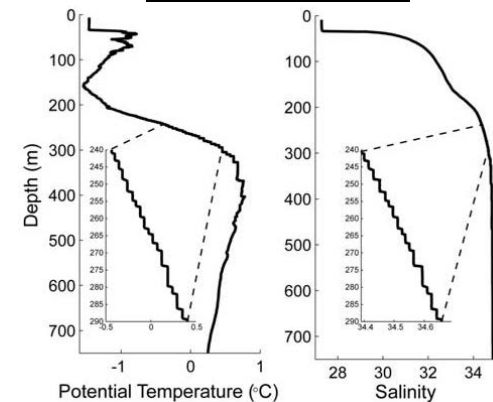


(Image: Timmermans et al. 2008)

# Modes

---

- For a nonuniform stratification, generally the modes need to be calculated numerically (the WKB method provides approximate solution, but not ideal).

$$w = W(z)e^{ikx} \rightarrow \frac{d^2W}{dz^2} + k^2 \left( \frac{N^2(z) - \omega^2}{\omega^2 - f^2} \right) W = 0.$$

- Still a Sturm-Liouville problem, so useful results apply, namely:
  - (i) Infinitely many solutions with wavenumber  $k_n$ ,
  - (ii) Modes are orthogonal,
  - (iii) Linear relations between physical variables persist, i.e.

$$U = \frac{i}{k} \frac{dW}{dz}; \quad V = \frac{f}{\omega k} \frac{dW}{dz}.$$

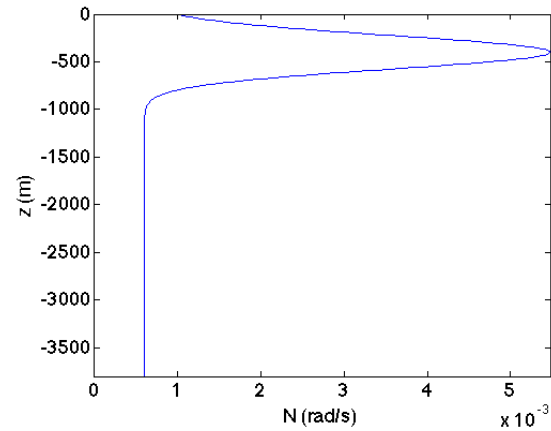
- Energy flux of mode  $n$ :  $E_n = \frac{u_n^2}{k_n} \frac{\rho_*(\omega^2 - f^2)}{2\omega}$ .
- General solution is a superposition of modes:  $w = \sum_n w_n W_n(z) e^{i(k_n x - \omega t)}$



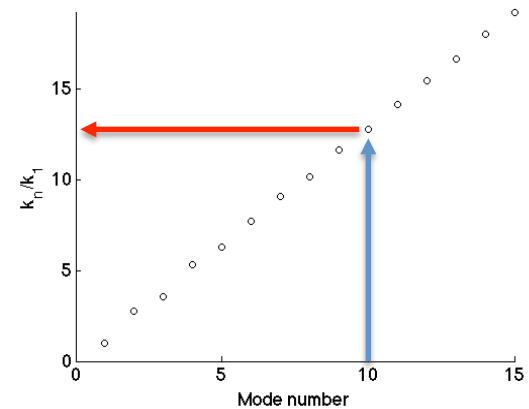
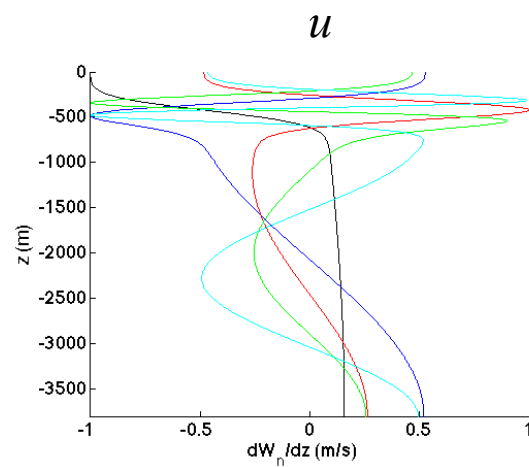
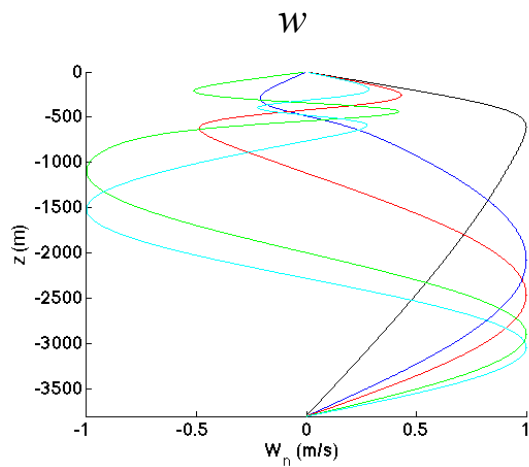
# Modes

- Consider reasonable model of an ocean stratification.

$$\begin{aligned}
 H &= 3800 \text{ m,} \\
 N_{\text{max}} &= 0.0055 \text{ rad/s,} \\
 N_{\text{deep}} &= 0.0006 \text{ rad/s,} \\
 f &= 0.0001046 \text{ rad/s.}
 \end{aligned}$$



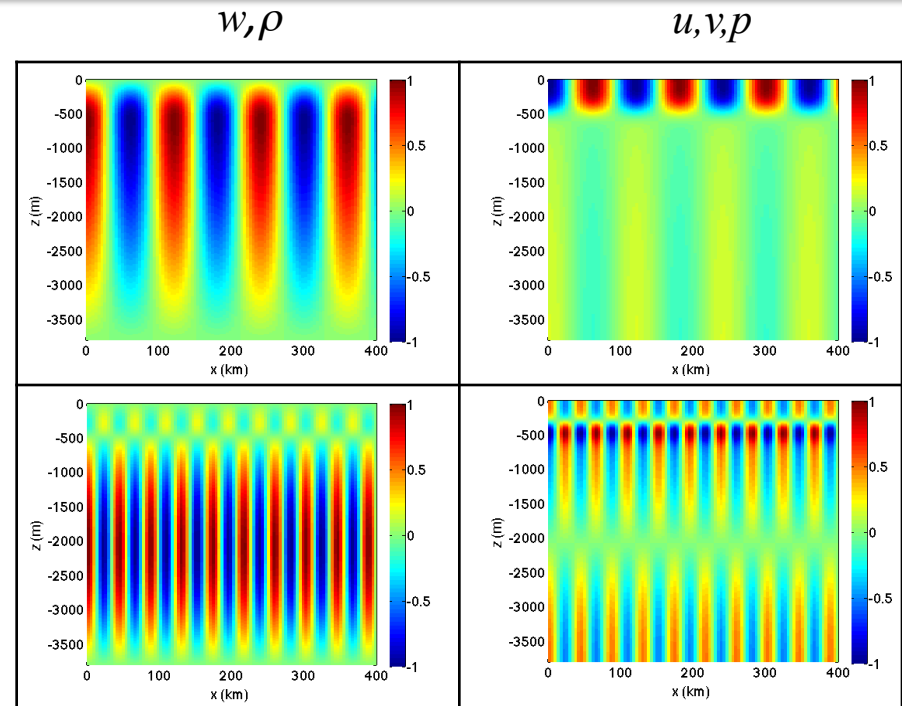
- The mode shapes, which are now a function of frequency, become biased towards the surface, and the horizontal wave numbers no longer satisfy  $k_n = nk_1$



# Wave fields

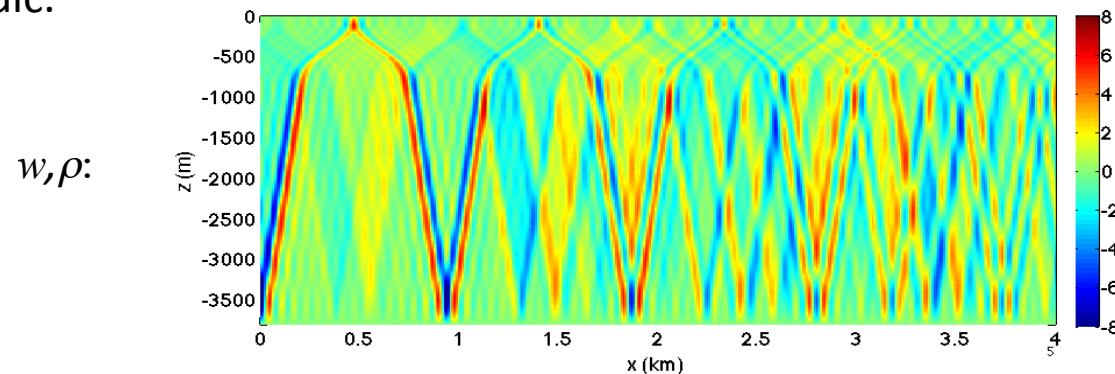
- Wave fields for the different vertical modes are manifest as follows:
- Horizontal wave lengths are on the order of 50-100km for modes 1 and 2, and phase speeds are on the order of 1m/s.

*Mode 1:*



*Mode 2:*

- Because of the nature of the wavenumber spectrum, a superposition of 15 modes is not spatially periodic.



# Modal decomposition

---

- Presented with a harmonic wave field, it is possible to extract the modal content.
- Provided the forcing frequency,  $\omega$ , stratification,  $N(z)$ , and background rotation,  $f$ , is known, the vertical modes and their wavenumbers,  $k_n$ , can be calculated.
- We exploit the fact that the measured wave field is assumed to be of the form:

$$u(x, z, t) = \sum_n u_n U_n(z) e^{i(k_n x - \omega t)}$$

- If a vertical profile of horizontal (or vertical) velocity is measured at two different times,  $t_1$  and  $t_2$ , at the same location,  $x_0$ , for example, the real and imaginary parts of the complex amplitude  $u_n$  can be determined from:

$$\begin{bmatrix} \text{Re}\{u_n\} \\ \text{Im}\{u_n\} \end{bmatrix} = \begin{bmatrix} \cos(k_n x_0 - \omega t_1) & -\sin(k_n x_0 - \omega t_1) \\ \cos(k_n x_0 - \omega t_2) & -\sin(k_n x_0 - \omega t_2) \end{bmatrix} \begin{bmatrix} \Gamma_n(x_0, z, t_1) \\ \Gamma_n(x_0, z, t_2) \end{bmatrix}$$

where

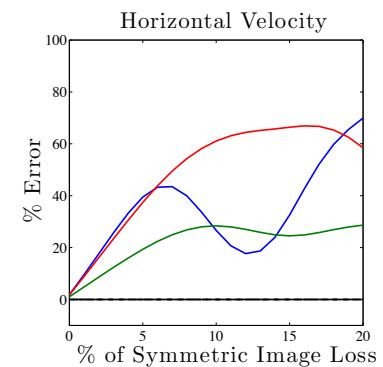
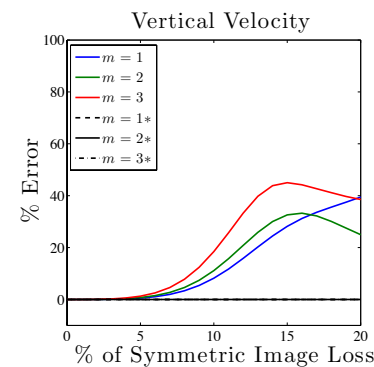
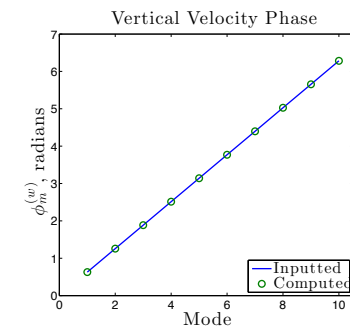
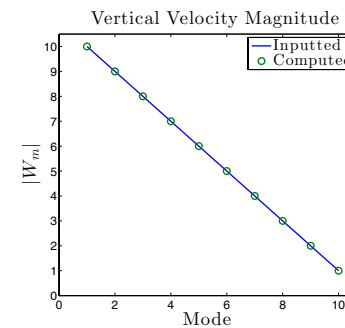
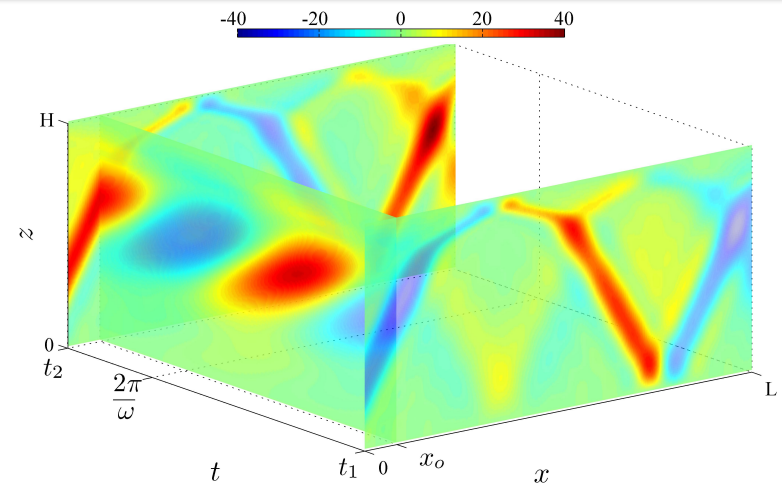
$$\vec{\Gamma}_{1,n}(x_0, z, t) = [\gamma_{n \times n}]^{-1} \times \int_{-H+\alpha}^{0-\beta} u(x_0, z, t) \vec{U}_{1,n}(z) dz \quad \text{and} \quad \gamma_{nm} = \int_{-H+\alpha}^{0-\beta} U_n(z) U_m(z) dz.$$

- The approach can do an excellent job even with incomplete information.

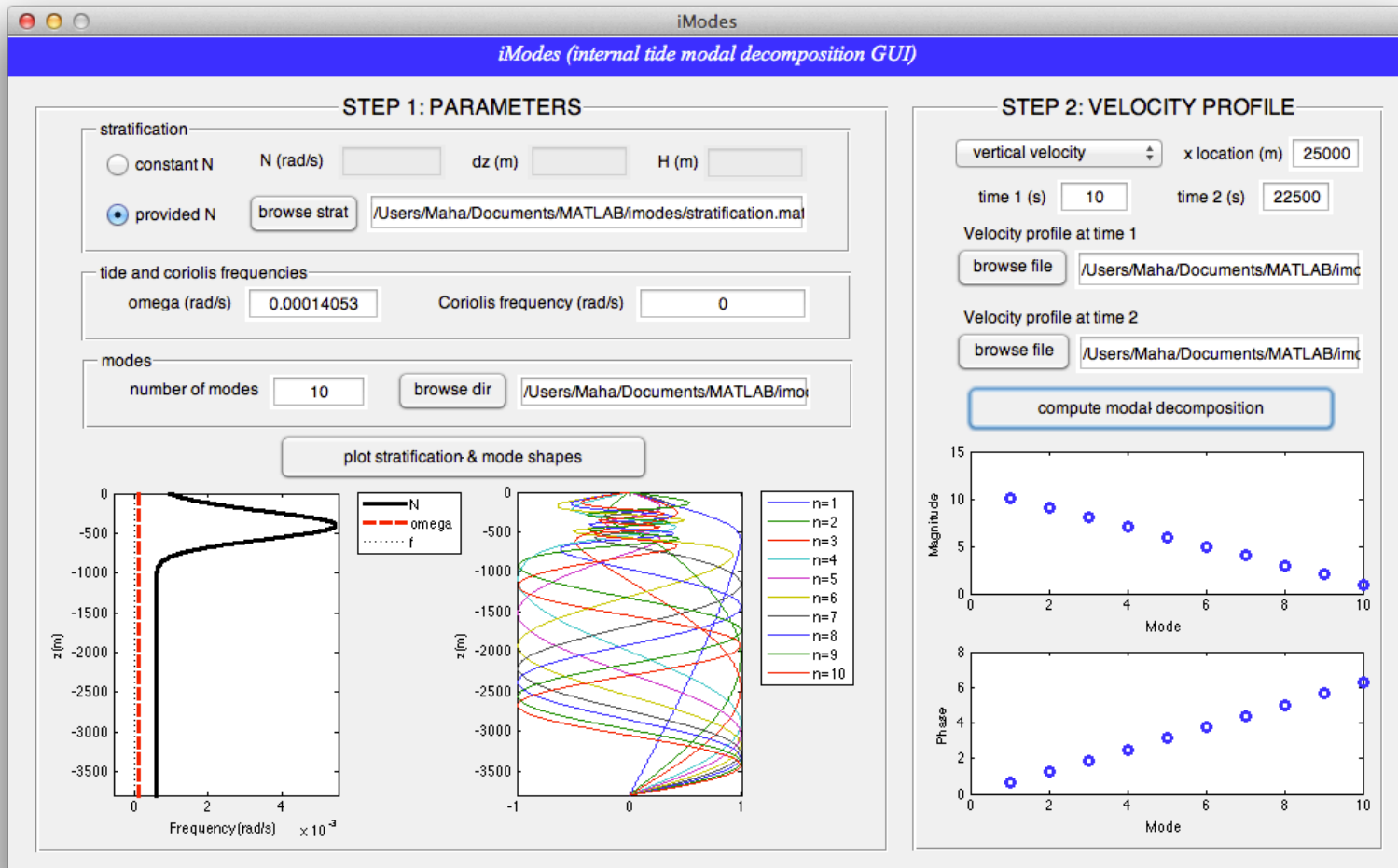


# Modal decomposition

- For our example stratification, we can start with a wave field comprising 10 modes with 10 different phases.
- By applying modal decomposition routines one can extract the modal amplitudes and phases.
- The method readily accounts for image loss up to 20% of the vertical domain (the key is to not lose all the information in the upper stratification).



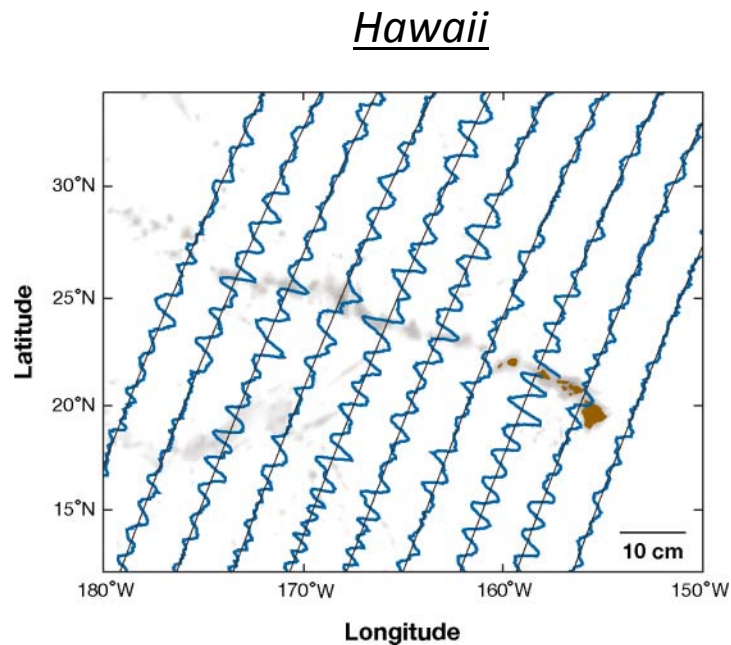
# iModes



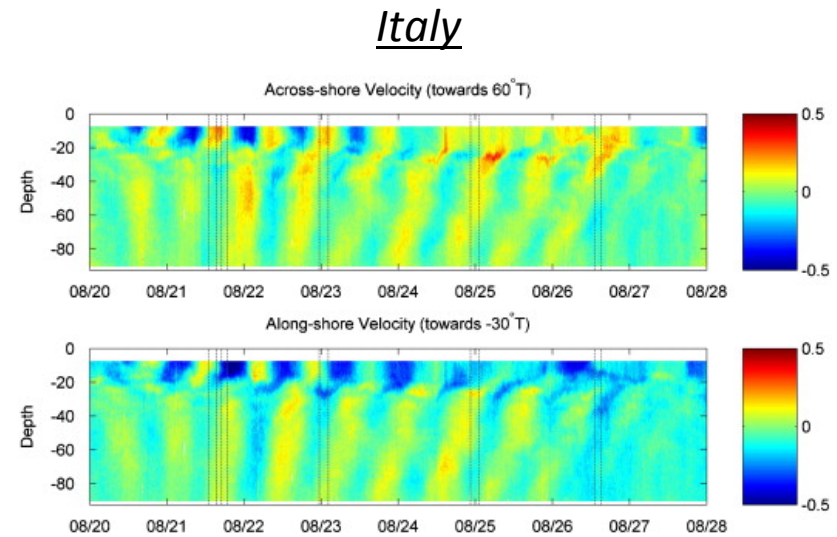
<http://web.mit.edu/endlab/downloads>

# Observations

- Are modes just an idealization only observed in analytical models? – No. There is clear observational evidence of propagating modes in the ocean.



- Surface displacement at M2 frequency is alternately reinforced and reduced by motions consistent with mode-1 and mode-2 wavelengths (*Ray & Mitchum 1997*).



- ADCP measurements of across shore and along shore components of velocity in the ocean water column of coast of Italy (*Carniel et al. 2012*).



# Generation

---



# Generation in the deep ocean

---

- There are currently understood to be two principle (linear) sources of internal wave energy flux into the deep ocean:

## 1. Flow past topography

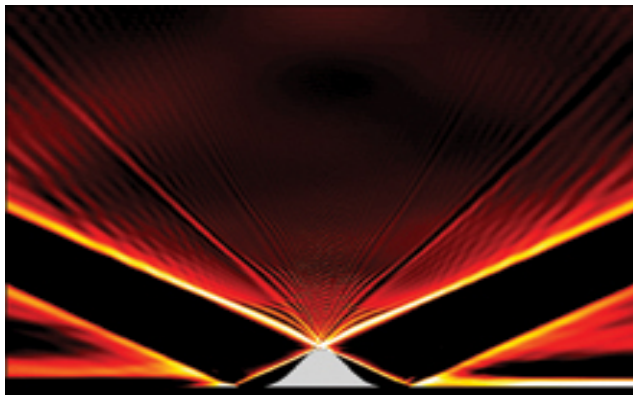


*(Image: Sarkar)*

## 2. Ocean surface forcing



*(Image: NASA)*

# Generation in the deep ocean

---

- There are currently understood to be two principle (linear) sources of internal wave energy flux into the deep ocean:

## 1. Flow past topography

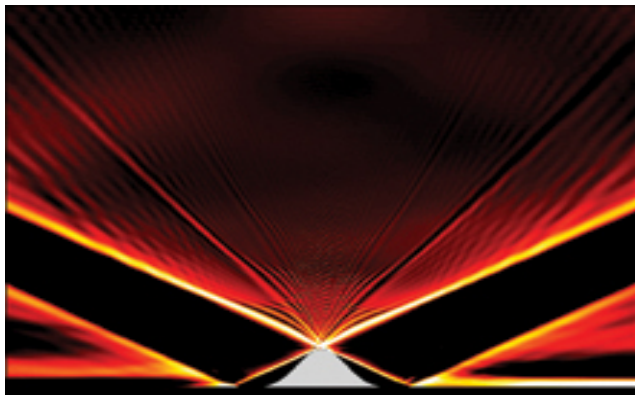


*(Image: Sarkar)*

## 2. Ocean surface forcing



*(Image: NASA)*

# Internal tides

- Barotropic (depth-independent) tides exist at frequencies such as:

*M2 - lunar, semi-diurnal = 12.42 hours*

*K1 - lunar, diurnal = 23.93 hours*

*S2 - solar, semi-diurnal = 12.00 hours*

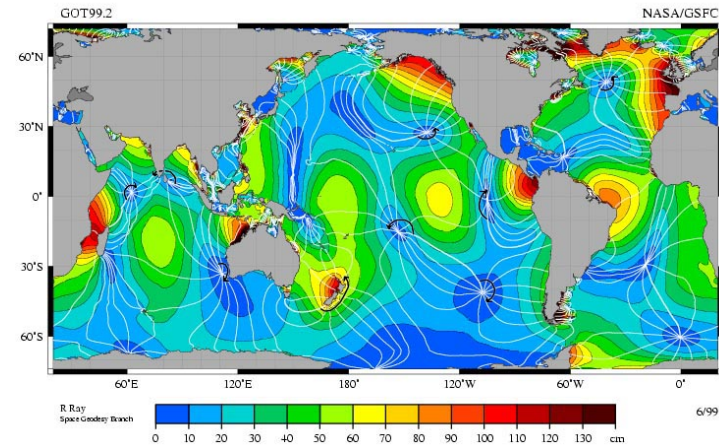


(Image: NASA/GSFC)

- The barotropic tides force the ocean to pass back and forth over ocean floor topography, disturbing the background stratification.

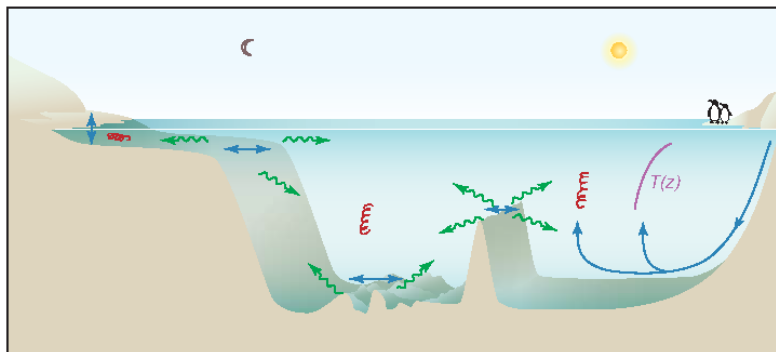


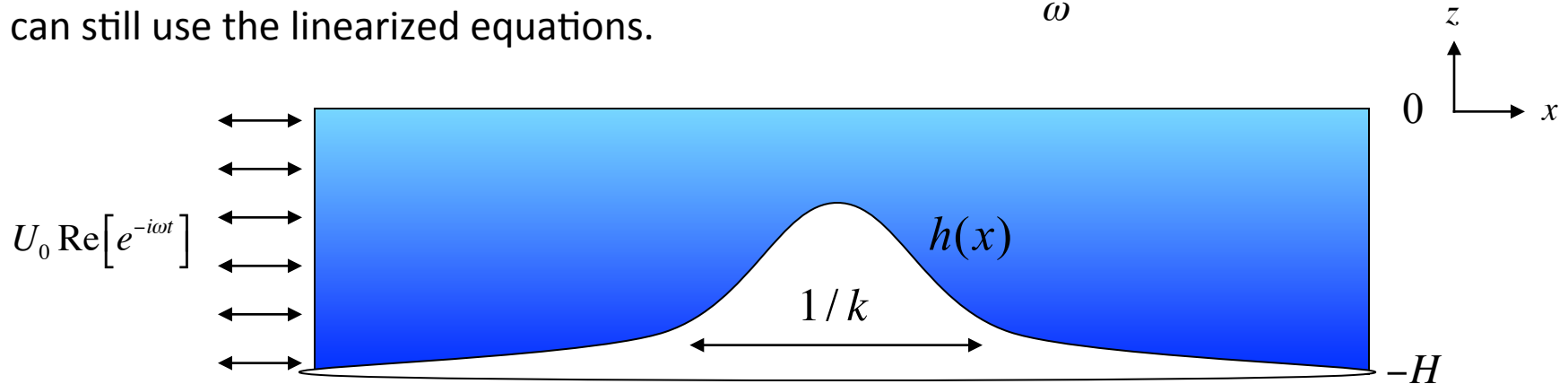
(Image: Garrett 2007)

video



# Linear model

- An important parameter is the tidal excursion parameter  $\frac{U_0 k}{\omega}$ ; provided this is small we can still use the linearized equations.



- It is convenient to work with the stream function:  $\psi = U_0 \text{Re}[\phi(x, z)e^{-i\omega t}]$  where  $(u, w) = \left(-\frac{\partial \psi}{\partial z}, \frac{\partial \psi}{\partial x}\right)$ .
- We decompose the flow into barotropic and baroclinic components:

$$\psi(x, z, t) = \psi_b(x, z, t) + \psi'(x, z, t) = \text{Re}[\phi_b(x, z)e^{-i\omega t}] + \text{Re}[\phi'(x, z)e^{-i\omega t}].$$

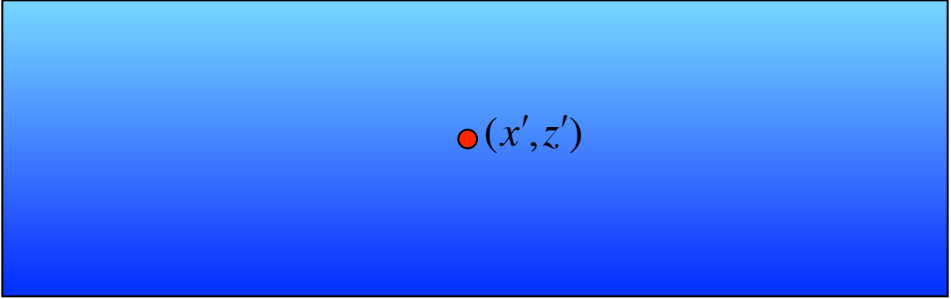
- The governing equation and boundary conditions for the perturbation wave field are:

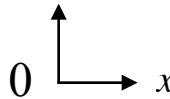
$$\left(\frac{N(z)^2 - \omega^2}{\omega^2 - f^2}\right) \frac{d^2 \phi'}{dx^2} - \frac{d^2 \phi'}{dz^2} = 0; \quad \phi'(x, 0) = -\phi_b(x, 0), \quad \phi(x, h(x)) = -\phi_b(x, h(x)).$$

# Point sources

---

- A starting point is to determine the wave field for a point source of internal wave energy at  $(x', z')$  subject to rigid boundary conditions at  $z = 0$  and  $z = -H$ :



$0$    $x$   
 $-H$

$$\left( \frac{N(z)^2 - \omega^2}{\omega^2 - f^2} \right) \frac{d^2 G}{dx^2} - \frac{d^2 G}{dz^2} = i\delta(x - x')(z - z').$$

- For a constant stratification,  $N$ , this equation is solved by separation of variables, giving:

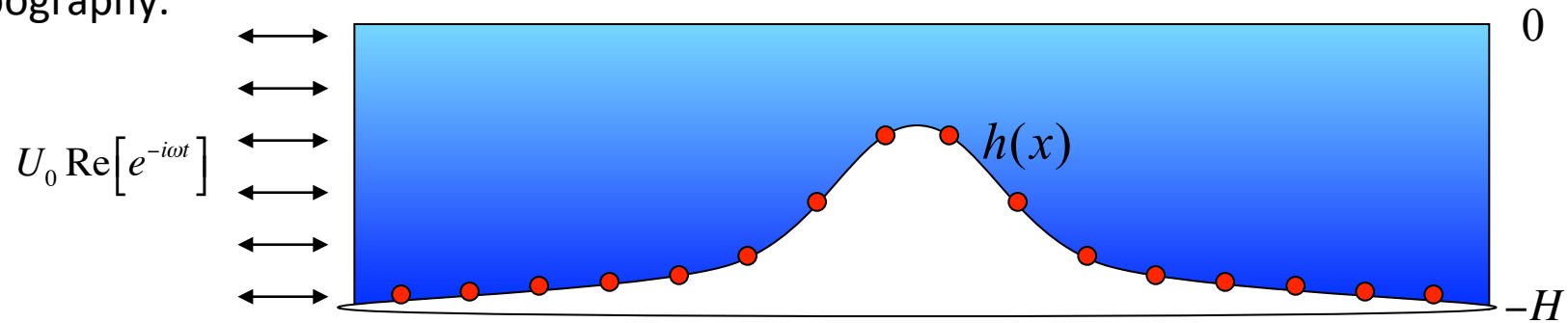
$$G(x - x')(z - z') = \sum_{n=1}^{\infty} \frac{1}{n\pi \tan \theta} \sin \frac{n\pi z'}{H} \sin \frac{n\pi z}{H} e^{i \frac{n\pi}{H \tan \theta} |x - x'|}.$$

- The Green's function is a sum over the vertical modes of the stratification

$$\omega^2 = N^2 \cos^2 \theta + f^2 \sin^2 \theta$$

# Topographic generation

- Robinson (1969) and Petrelis *et al.* (2006) proposed that the wave field generated can be attributed to the sum of waves emitted from a distribution of point sources on the topography.



- Mathematically, we write this as:  $\phi(x, z) = \int_{x_1}^{x_2} \gamma(x') G(x, x', z, h(x')) dx'$ .
- Since the wave field generated by point sources already satisfies the internal wave equation, all that remains is to satisfy the boundary conditions.
- The top boundary condition (rigid lid) is also already satisfied. The bottom boundary condition reduces to the following:

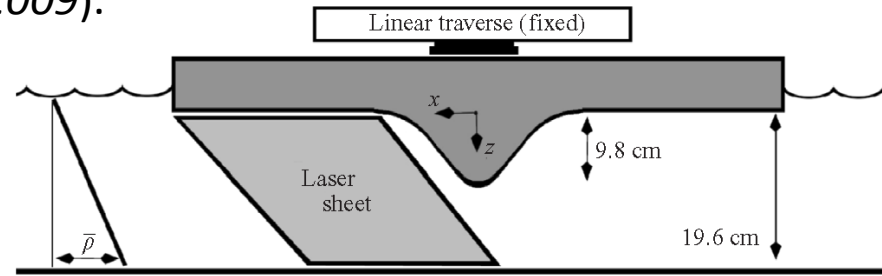
$$\phi(x, h(x)) = \int_{x_1}^{x_2} \gamma(x') G(x, x', h(x), h(x')) dx' = -\phi_b(x, h(x)) = U_0 h(x).$$

- Discretize integral in  $x$  and choose how many modes  $n$  to represent Green's function (see, for example, Echeverri & Peacock (2010))

# Validation

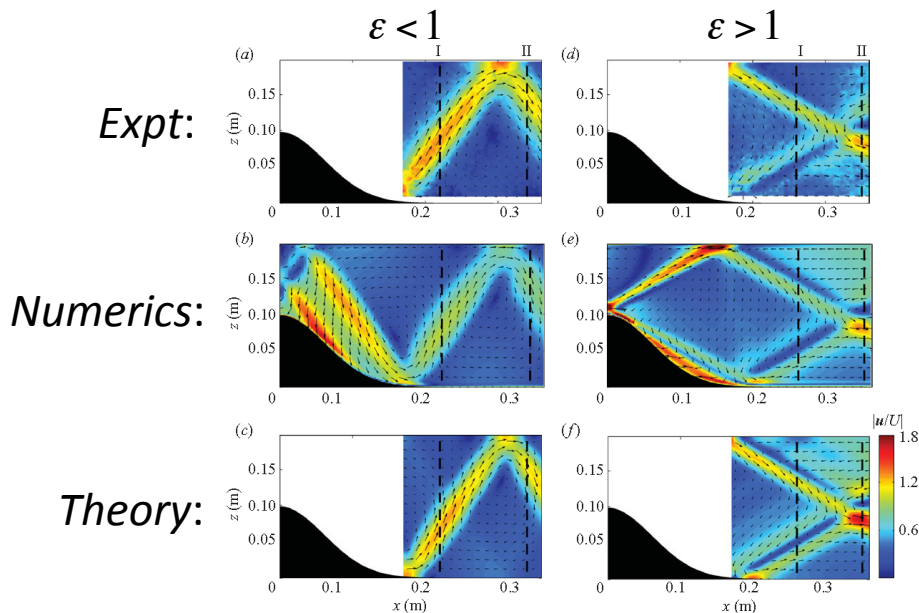
- To test the method, comparisons were made between theory, laboratory experiments and numerical simulations (Echeverri *et al* 2009).

- Experiments were performed in the frame of reference of the barotropic tide.

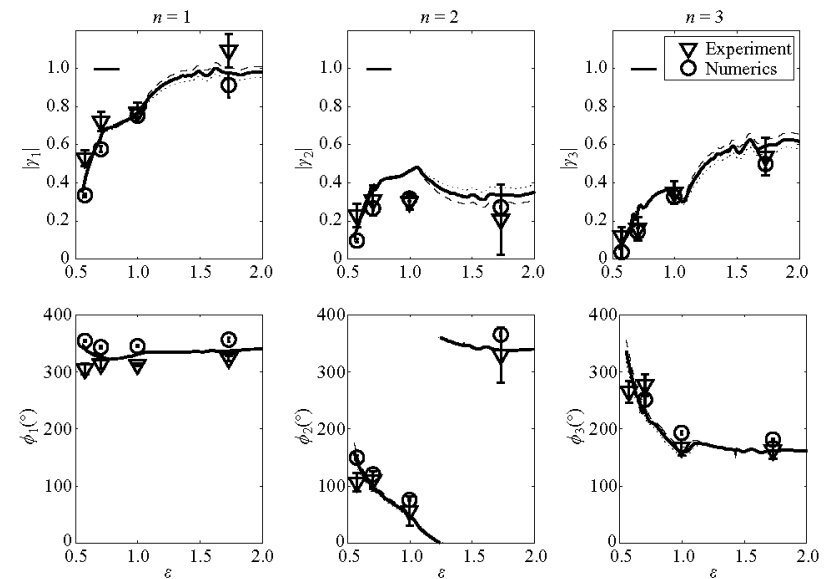


- Very good agreement for sub- ( $\varepsilon < 1$ ) and super-critical ( $\varepsilon > 1$ ) wave fields.  $\left( \varepsilon = \frac{\text{topographic slope}}{\text{internal ray slope}} \right)$

## Visualizations



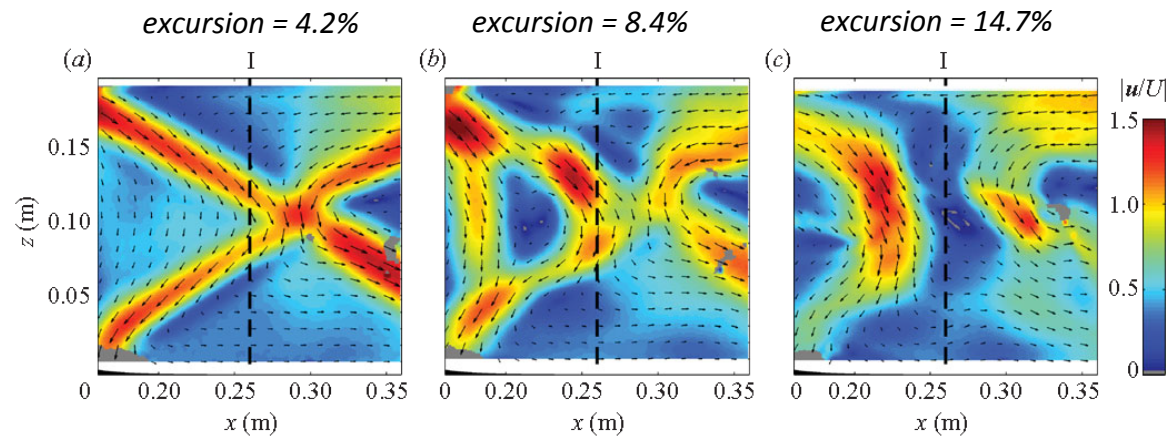
## Modal decomposition



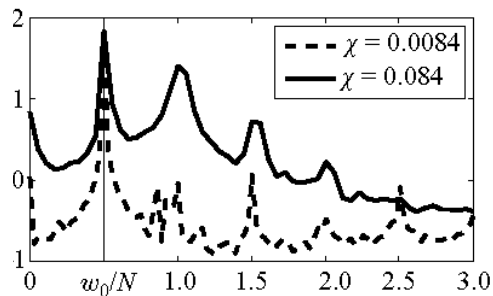


# Nonlinear regimes

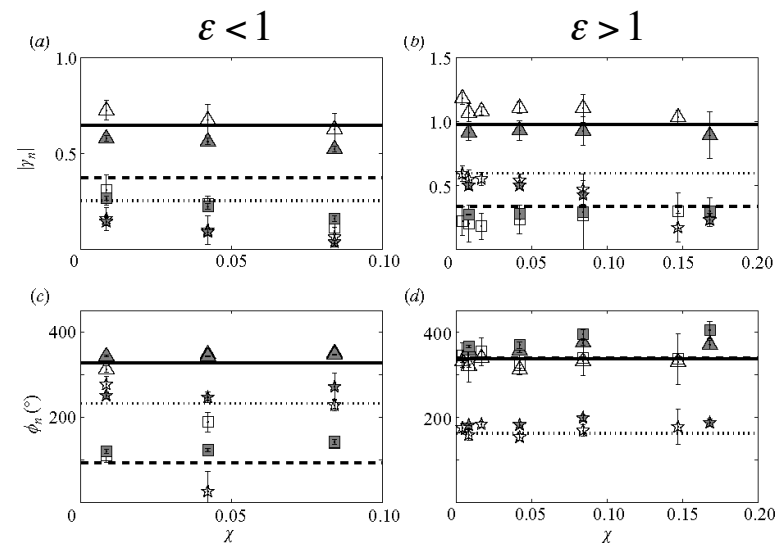
- By increasing the amplitude of oscillation of the topography (and thus the tidal excursion parameter), the wave field becomes increasingly nonlinear.



- Additional harmonics are evident in a vertically average FFT spectrum.

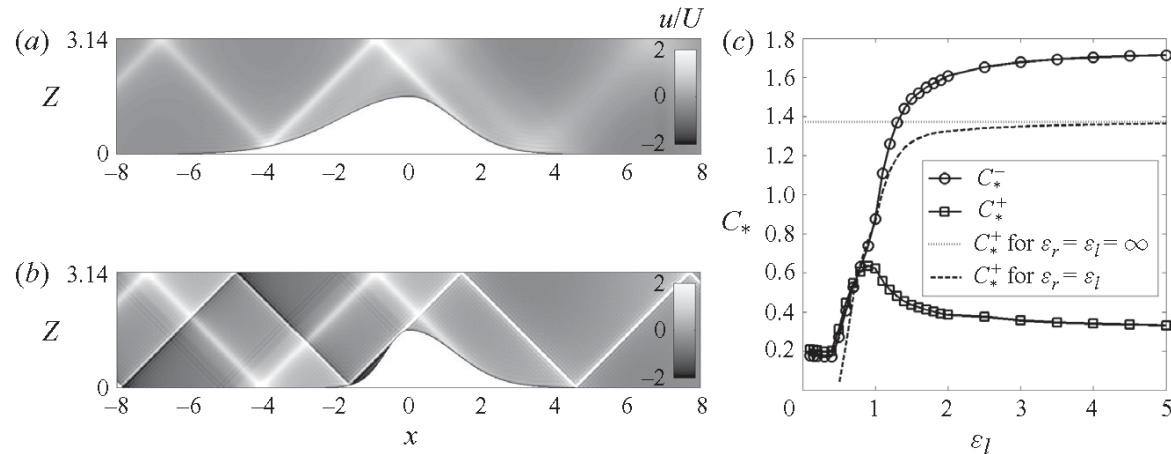


- Nevertheless, the linear model still does a remarkably good job.

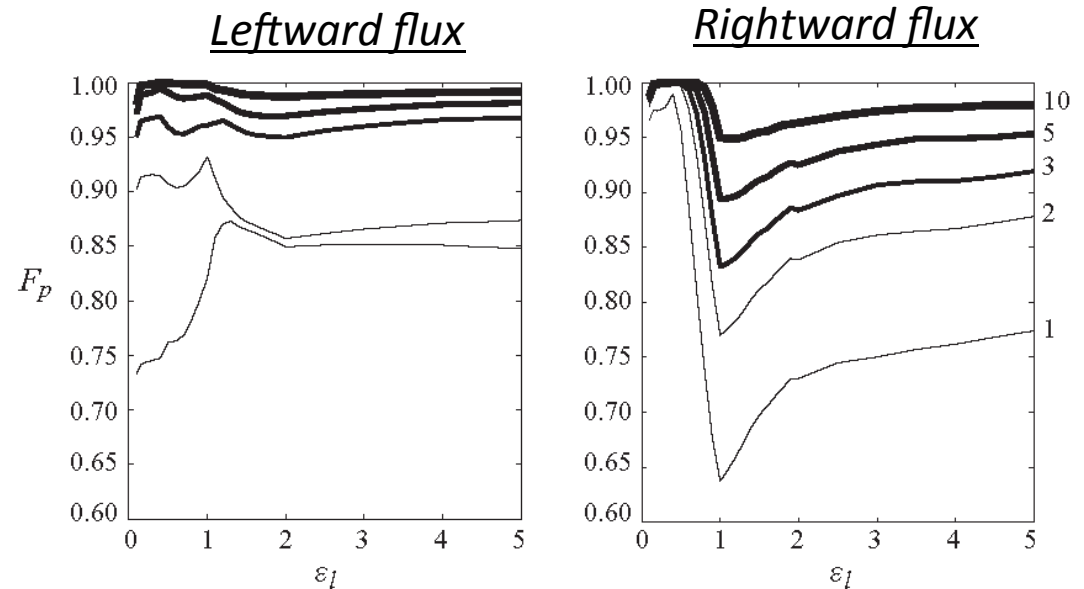


# Isolated ridge

- Further use of the theoretical method reveals the nature of internal tide generation by isolated ridges.

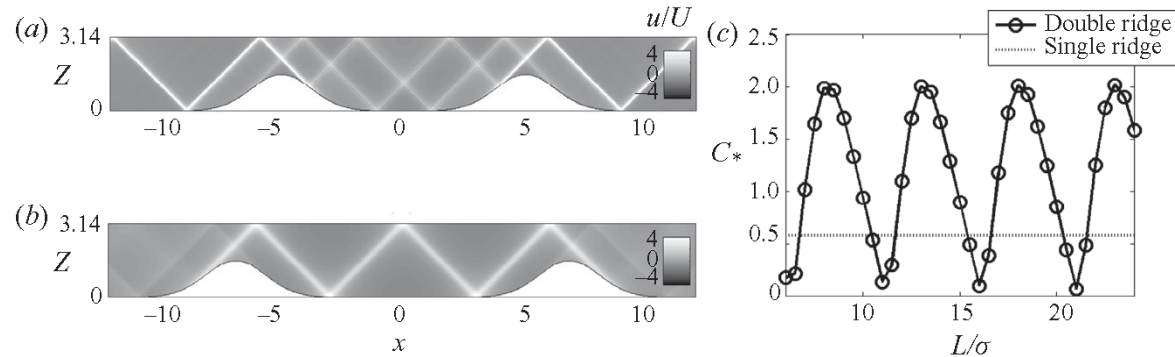


- The modal structure of the radiated wave fields can also be investigated.
- Both the leftward and rightward energy fluxes are dominated by mode 1.

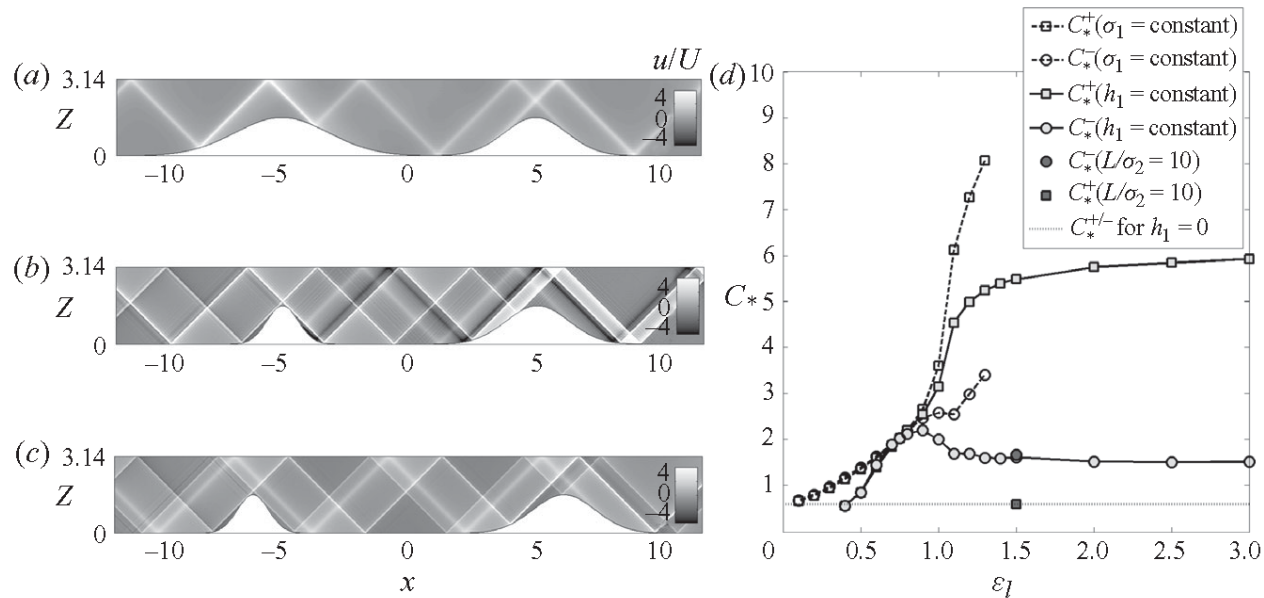


# Double ridge

- The presence of multiple ridges can have a profound (and complex) impact on the radiated wave field.



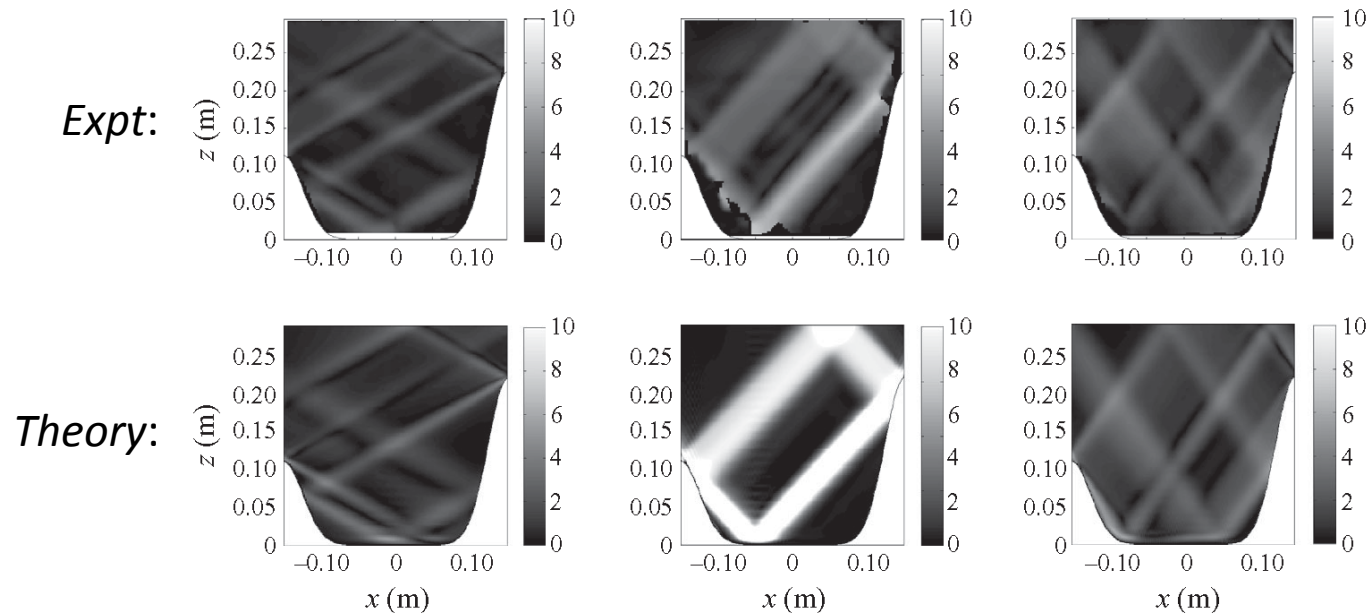
- Both criticality and relative location play key roles, making it difficult to anticipate results.



# Attractors

---

- There is the interesting scenario that ridges can trap wave energy giving internal wave attractors.
- The idea of an internal wave attractor was first realized by Maas *et al.* (1997).
- The linear theory is able to reliably predict the existence of internal tide attractors.



- While it may seem somewhat idealized, there is evidence that these ideas are relevant to the Luzon Strait double ridge system in the South China Sea.



# Real stratifications

---

- A recent advance enables the Green function method to be extended to arbitrary nonuniform stratifications (Mathur, Carter & Peacock 2012).
- What makes this possible is that for a nonuniform stratification, the Green function can be expressed as a sum over the vertical modes:

$$G(x, x', z, z') = \sum_{p=1}^{p=\infty} \frac{\Phi_p(z')}{2k_p} \left( \int_{-H}^0 \left( \frac{N^2(z) - \omega^2}{\omega^2 - f^2} \right) \Phi_p^2 dz \right)^{-1} e^{ik_p|x-x'|} \Phi_p(z)$$

recalling that the vertical modes  $\Phi_p$  are obtained by numerically solving (subject to rigid lid boundary conditions):

$$\Phi_{p,zz} + \left( \frac{N^2(z) - \omega^2}{\omega^2 - f^2} \right) k_p^2 \Phi_p = 0.$$

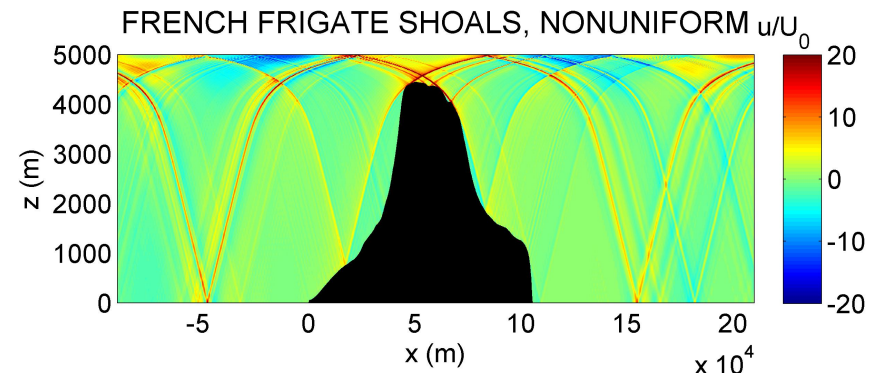
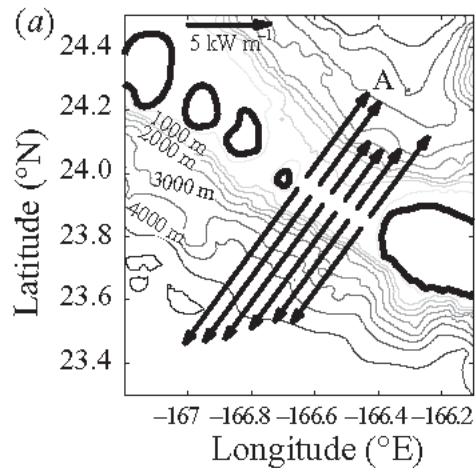
- The internal wave problem is again solved by imposing the bottom boundary condition:

$$\int_{x_1}^{x_2} \gamma(x') G(x, x', h(x), h(x')) dx' = U_0 h(x).$$

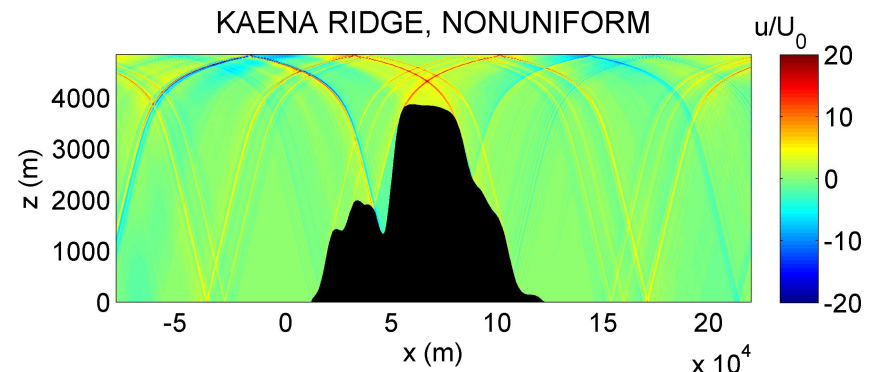
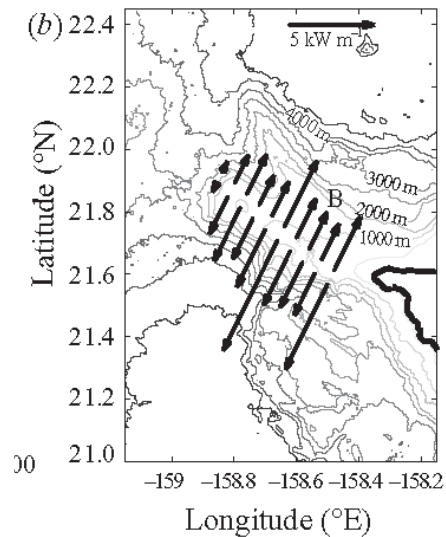
# Nonuniform stratifications

- Using this approach, it is possible to calculate the internal tide generated by two-dimensional cross sections of realistic topography in realistic stratifications.
- We use the Hawaiian ridge as an example.

*French Frigate Shoals:*



*Kaena Ridge:*



Echeverri & Peacock (2010), Mathur, Carter & Peacock (2013)

# iTides

The screenshot shows the iTides GUI with the following sections:

- STEP 1: PARAMETERS**
  - topography:** A text box containing the path `/Users/mmercier/Documents/travail/PostDoc/iTides/iTides` and a `browse topo` button.
  - stratification:** Two radio buttons: `constant N` (unselected) and `provided N` (selected). The `provided N` section includes a `browse strat` button and a text box with the same path as above. There are also input fields for `N (rad/s)` and `dz (m)`.
  - tide and coriolis frequencies:** Two input fields containing the values `0.4` and `0.1`.
  - A `plot topo & strat` button is located below the stratification section.
- STEP 2: GAMMA DISTRIBUTION**
  - A dropdown menu set to `barotropic` and an input field containing `500`.
  - A text box for "Specify output filename (default taken otherwise)" containing `output_gamma`.
  - A `gamma_distribution` button.
- STEP 3: WAVEFIELD**
  - computation:** Input fields for `u0 (m/s)`, `rho0 (kg/m^3)` (value `50`), and `dx (m)` (value `2`). A `viscous correction` checkbox is checked.
  - A text box for "Specify output filename (default taken otherwise)" containing `wavefield`.
  - A `compute wavefield` button.
  - display:** A dropdown menu set to `horizontal velocity` and an input field containing `phase (rad)`.
  - A `display_wavefield` button.

At the bottom of the STEP 1 section, there are two plots:

- The left plot shows the topography profile  $z$  (m) versus  $x$  (m). The vertical axis ranges from 0 to -0.45, and the horizontal axis ranges from -1.5 to 1.5. The plot shows a wave-like profile with two peaks.
- The right plot shows the stratification profile  $N$  (rad/s) versus  $x$  (m). The vertical axis ranges from 0 to -0.45, and the horizontal axis ranges from 0 to 1. The plot shows a curve that starts at 0, drops to a minimum, and then rises to a maximum. A vertical dashed red line is at  $x = 0.5$ , and a vertical dotted black line is at  $x = 0$ .

<http://web.mit.edu/endlab/downloads>

# Three-dimensionality

- So what about the fact that topography in the real ocean is three-dimensional?

## Theory

Theoretical modeling for ideal shapes, such as sphere (Voisin 2003) and pillbox (Baines 2007).

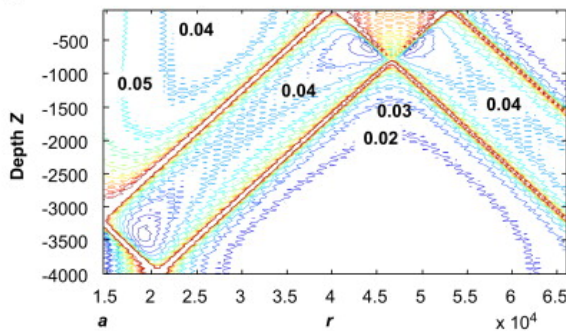


(Image: Baines 2007)

## Experiments

Limited research only in recent years (e.g. Gaussian seamount, King *et al.* 2010).

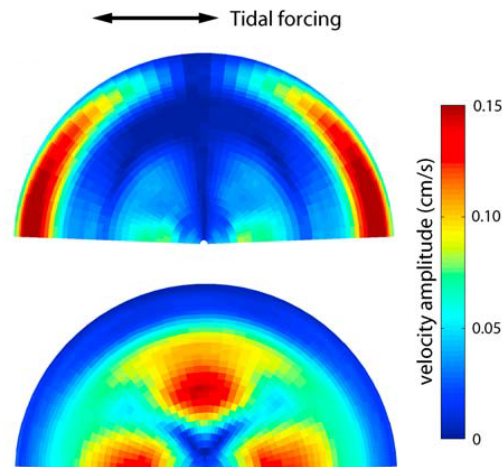


(Image: King *et al.* 2010)

## Numerics

Fundamental modeling, e.g. Holloway & Merrifield (1999), Munroe & Lamb (2005).

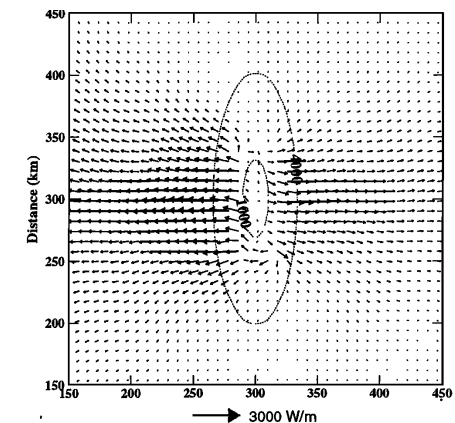


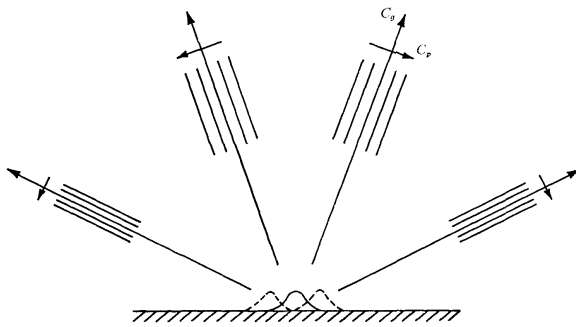
(Image: Holloway & Merrifield 1999)

- Ridges with a horizontal aspect ratio 3:1 produces an energetic internal tide, nearly an order of magnitude than for similar sized seamounts (40 times larger for a ridge).
- An analytic estimate of the energy flux from all seamounts is 2.4GW (comparable to just the Hawaiian Ridge system).



# Finite excursion

- Internal waves need not be generated at the tidal forcing frequency.
- This is apparent when the tidal excursion parameter is large, for example, resulting in the generation of “lee-waves”, which is not uncommon in shallower coastal waters with smaller topography.
- The classic “linear” analysis of this scenario is that of *Bell (1975)* – retain  $\vec{U}_0 \cdot \nabla \vec{u}$



- As excursion parameter is increased, harmonics of the forcing frequency are excited:  $\omega = n\omega_0$
- In the limit of very large excursion parameter, the lee wave frequency dominates:  $\omega = U_0 k$

- These nonlinear waves are readily seen in numerics and experiments.

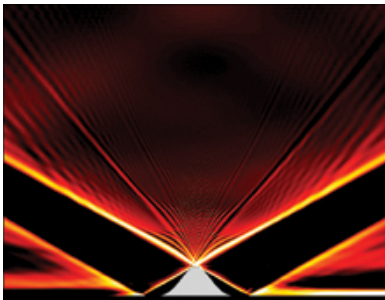


(Image: Rapaka et al 2013)

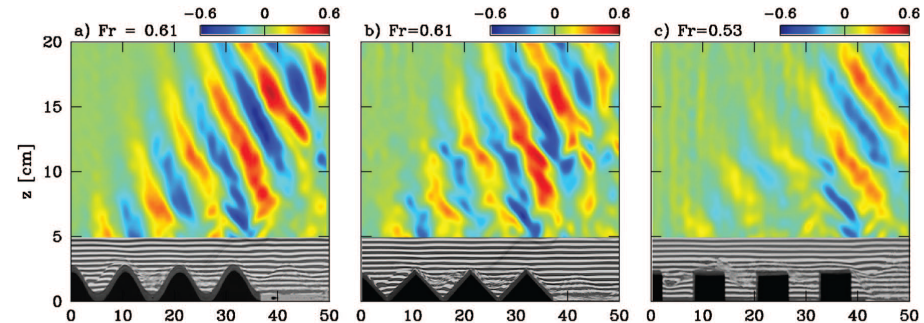
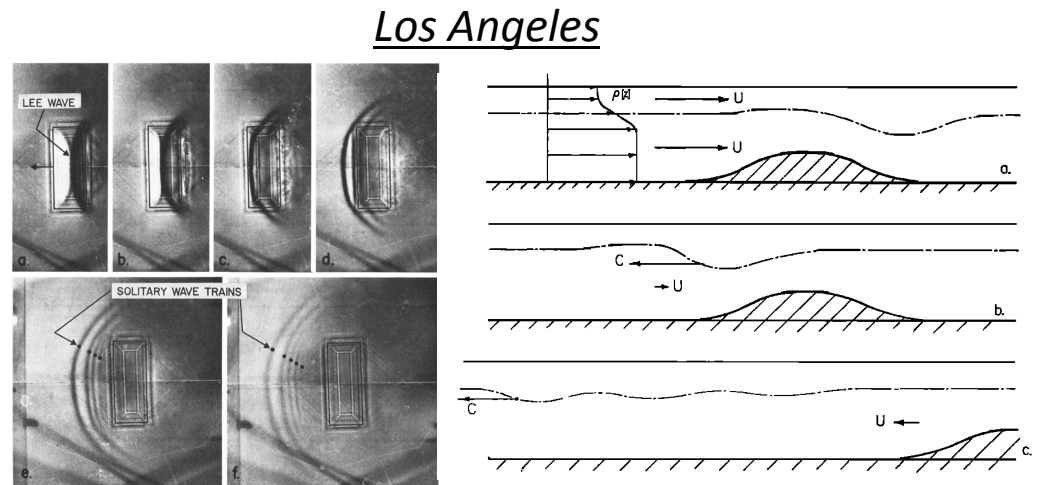


(Image: Aguilar & Sutherland 2006)

- The contribution of lee waves to the global energy budget is not expected to be significant (although there is still some more work to be done regarding the ACC).

# Nonlinear generation

- When tidal flow speed  $U_0$  exceeds the modal internal wave phase  $c_p$  speed (i.e.  $Fr = U_0/c_p > 1$ ), nonlinear internal waves arise at the generation site.
- An example of this was demonstrated in lab experiments by Maxworthy (1979).



(Images: Maxworthy 1979)

- Related phenomenon are observed at many different global locations.
- Although locally dramatic, it is believed the energetics are such that this is not a significant contribution to the global energy budget.

## Knight Inlet, British Columbia

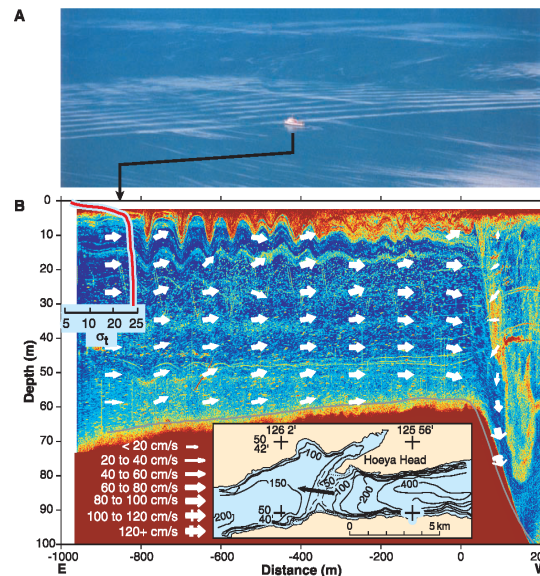


(Image: Farmi & Armi 1999)

## Straits of Gibraltar



(Image: ERS 2006)

# Field programs

- Several major field experiments have focused on internal tide generation, a pioneering one in the US being the Hawaiian Ocean Mixing Experiment (HOME).

- Comparison of observed and predicted energy fluxes.

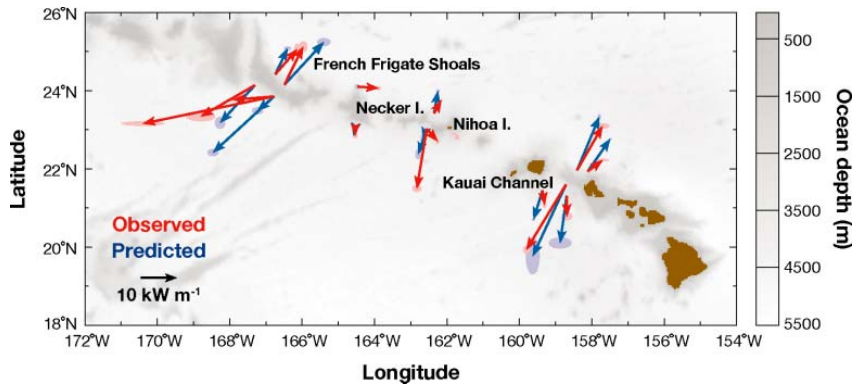


(Image: Rudnick et al 2003)

- 300m amplitude waves on the ridge flank.

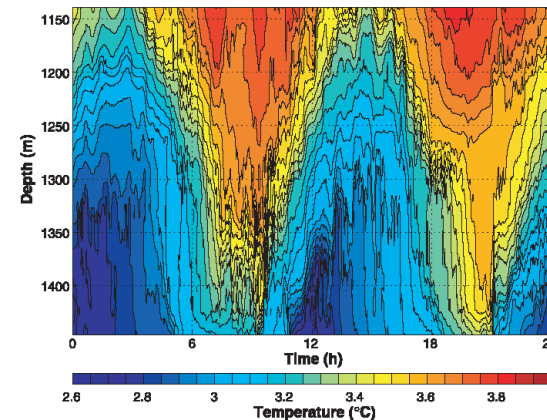


(Image: Rudnick et al 2003)

- Beams of internal tidal energy radiating from the vicinity of the Kaena ridge crest.

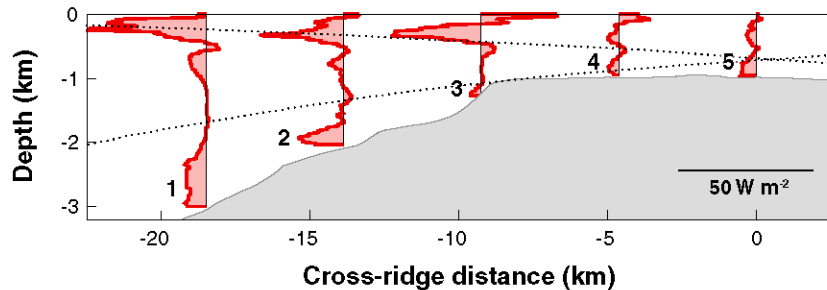


(Image: Nash et al 2006)

- Low modes dominate the downslope energy flux.

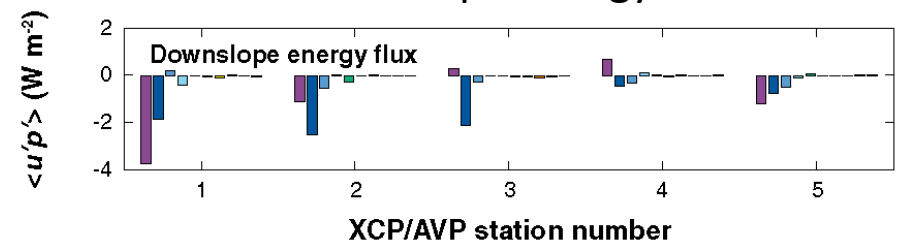
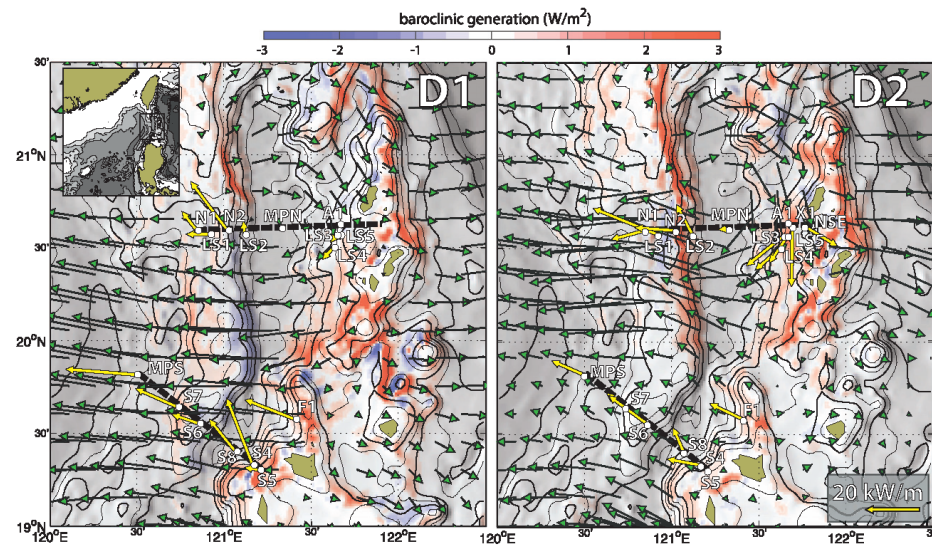
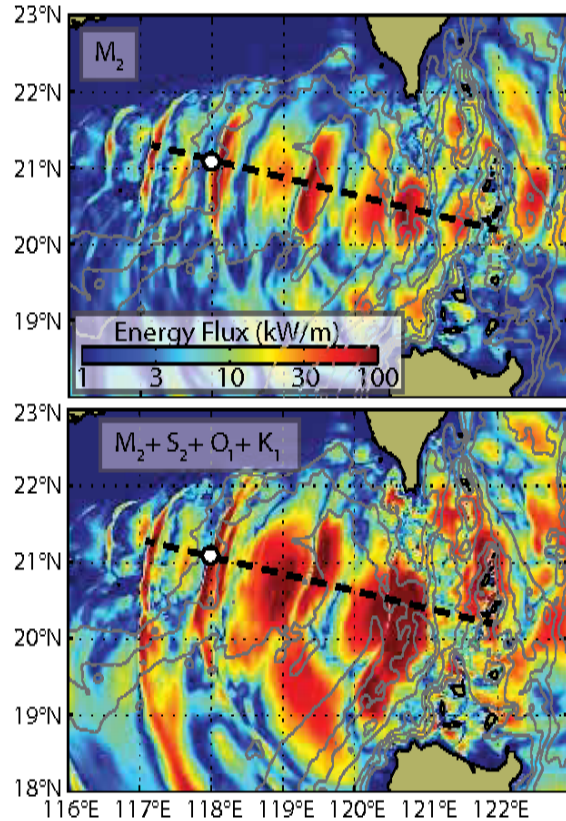


(Image: Nash et al 2006)



# Field programs

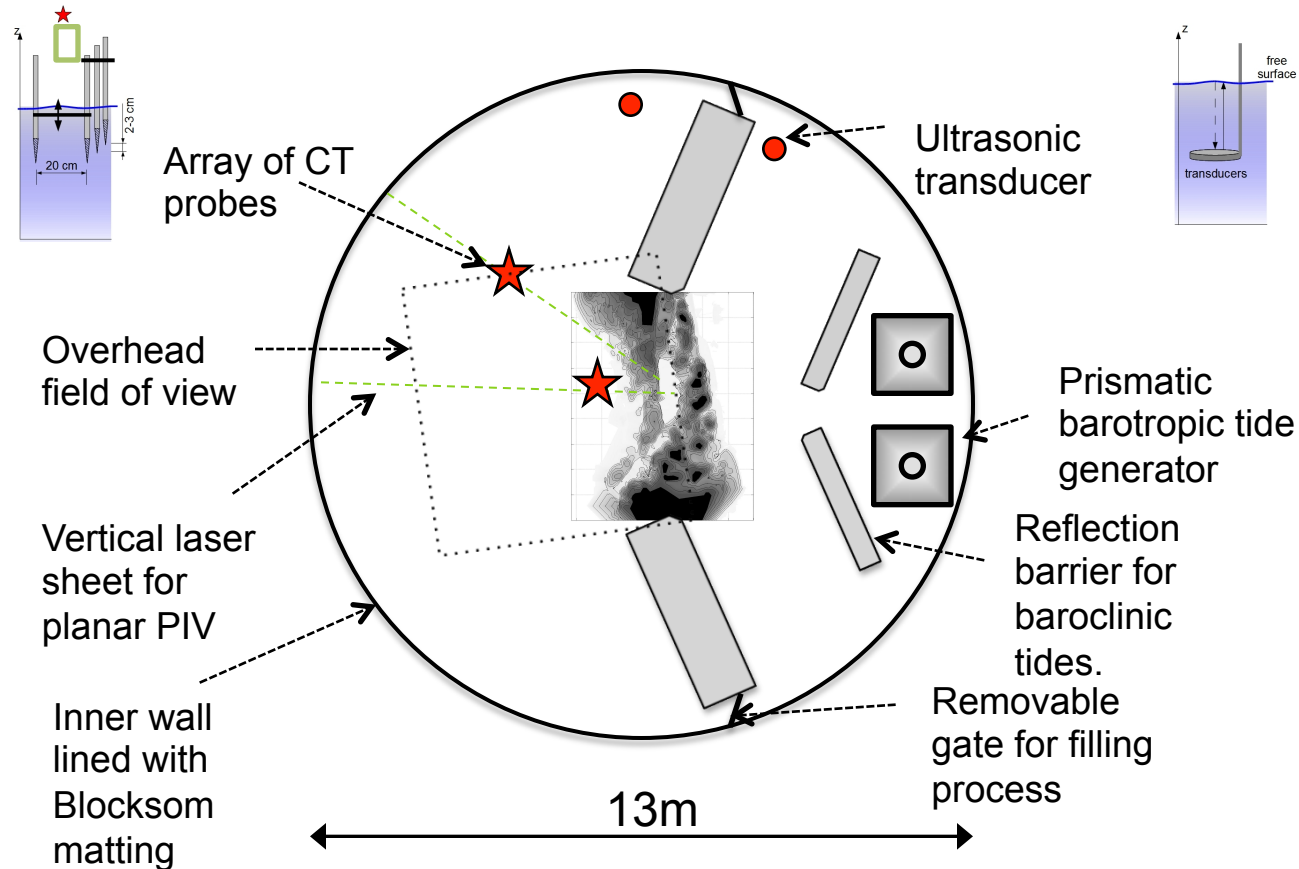
- Another major research program is the Internal Waves In Straits Experiment (IWISE) in the South China Sea.
- While 2D analysis gives some insight into the generation, the complexity of the topography means that this is really a 3D generation problem.



(Images: Alford et al 2011)

# Coriolis experiment

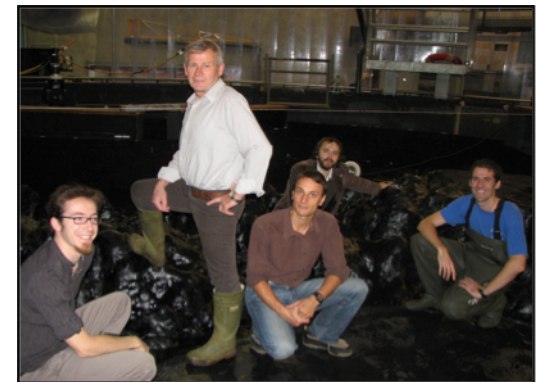
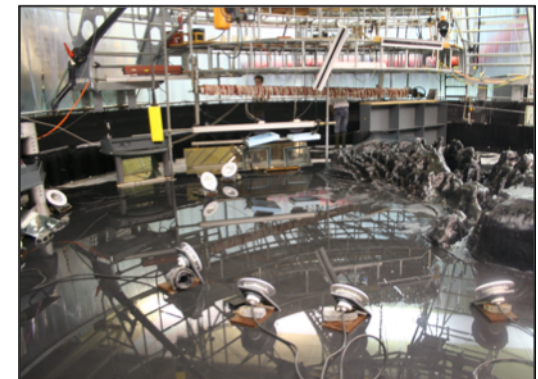
- As part of the IWISE program we performed “the most ambitious laboratory experimental study of internal tide generation of all time” (?).



- Key challenges to overcome were: (i) Achieving dynamic similarity with the ocean, (ii) Constructing the experiment, (iii) Obtaining data.



# Coriolis experiment



# Coriolis experiment

- Dynamical similarity:

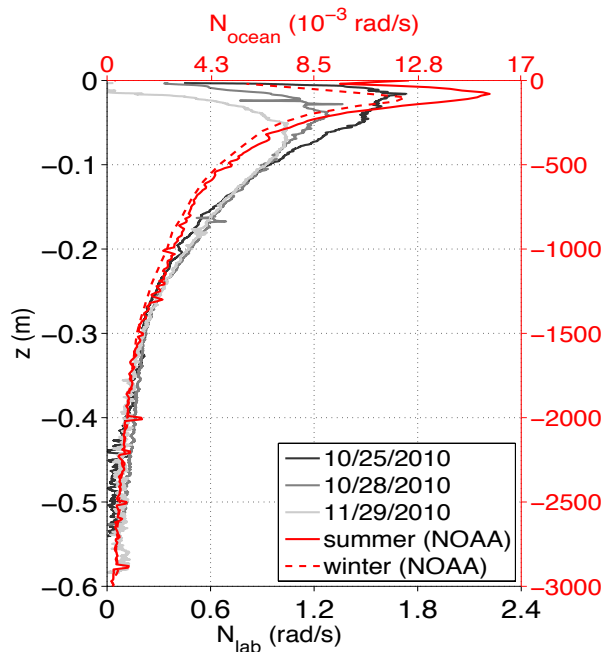
10 dimensional parameters:

	$\omega$ (rad/s)	$f$ (rad/s)	$N_m$ (rad/s)	$N_b$ (rad/s)	$U$ (m/s)	$\delta$ (m)	$H$ (m)	$L$ (m)	$h_0$ (m)	$\nu$ (m <sup>2</sup> /s)
<i>Luzon</i>	$1.40 \cdot 10^{-4}$	$5.00 \cdot 10^{-5}$	$1.57 \cdot 10^{-2}$	$3.65 \cdot 10^{-4}$	0.1	100	$3.0 \cdot 10^3$	$1.0 \cdot 10^5$	$1.5 \cdot 10^3$	$10^{-6}$
<i>Batan</i>	$1.40 \cdot 10^{-4}$	$5.00 \cdot 10^{-5}$	$1.57 \cdot 10^{-2}$	$1.28 \cdot 10^{-3}$	1.0	100	$1.5 \cdot 10^3$	$1.0 \cdot 10^4$	$8.0 \cdot 10^2$	$10^{-6}$
×	$2.76 \cdot 10^3$	$2.76 \cdot 10^3$	$1.41 \cdot 10^2$	$1.41 \cdot 10^2$	$2.76 \cdot 10^{-2}$	$5 \cdot 10^3$	$5 \cdot 10^3$	$10^5$	$5 \cdot 10^3$	1
<i>Lab<sub>L</sub></i>	$3.86 \cdot 10^{-1}$	$1.38 \cdot 10^{-1}$	2.21	$5.15 \cdot 10^{-2}$	$2.76 \cdot 10^{-3}$	0.02	0.6	1.0	0.30	$10^{-6}$
<i>Lab<sub>B</sub></i>	$3.86 \cdot 10^{-1}$	$1.38 \cdot 10^{-1}$	2.21	$1.80 \cdot 10^{-1}$	$2.76 \cdot 10^{-2}$	0.02	0.3	0.1	0.16	$10^{-6}$

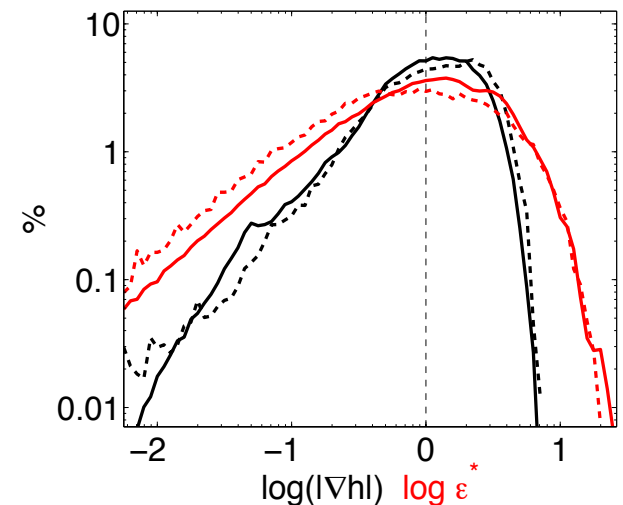
8 dimensionless parameters:

	$h^*$	$\delta^*$	$N^*$	$\epsilon^*$	$A^*$	$Re^*$	$Ro^*$	$Lo^*$	$Fr_1^*$	$Fr_2^*$
<i>Luzon</i>	0.50	$3.3 \cdot 10^{-2}$	43.0	$[4 \cdot 10^{-3} - 1.4 \cdot 10^1]$	$7.1 \cdot 10^{-3}$	$1.0 \cdot 10^{10}$	$2.0 \cdot 10^{-2}$	$2.5 \cdot 10^{-2}$	$3.6 \cdot 10^{-2}$	$7.3 \cdot 10^{-2}$
<i>Batan</i>	0.53	$6.6 \cdot 10^{-2}$	12.3	$[4 \cdot 10^{-3} - 1.4 \cdot 10^1]$	$7.1 \cdot 10^{-1}$	$1.0 \cdot 10^{10}$	2.0	$2.7 \cdot 10^{-1}$	$4.2 \cdot 10^{-1}$	$8.3 \cdot 10^{-1}$
×	1	1	1	1	1	$2.76 \cdot 10^{-7}$	1	0.98	1	1
<i>Lab<sub>L</sub></i>	0.50	$3.3 \cdot 10^{-2}$	43.0	$[1 \cdot 10^{-2} - 1.4 \cdot 10^1]$	$7.1 \cdot 10^{-3}$	$2.8 \cdot 10^3$	$2.0 \cdot 10^{-2}$	$2.4 \cdot 10^{-2}$	$3.6 \cdot 10^{-2}$	$7.3 \cdot 10^{-2}$
<i>Lab<sub>B</sub></i>	0.53	$6.6 \cdot 10^{-2}$	12.3	$[1 \cdot 10^{-2} - 1.4 \cdot 10^1]$	$7.1 \cdot 10^{-1}$	$2.8 \cdot 10^3$	2.0	$2.6 \cdot 10^{-1}$	$4.2 \cdot 10^{-1}$	$8.3 \cdot 10^{-1}$

Stratification:



Bathymetry:





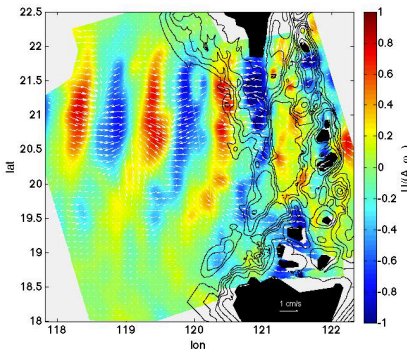
# Coriolis experiment

- The M2 internal tide, whose wavelength is comparable to the ridge separation, is significantly shaped by the topography.
- The K1 internal tide, being longer wavelength, is less impacted by the shape of the ridge system.
- The vertical structure of the radiated internal tide is dominated by mode 1.

Snapshot

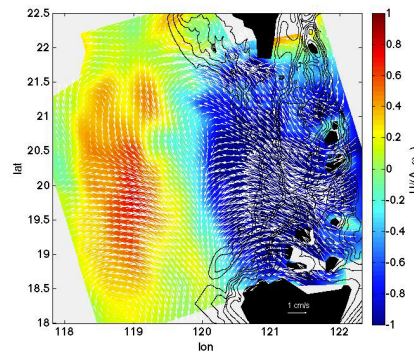
Phase

M2:



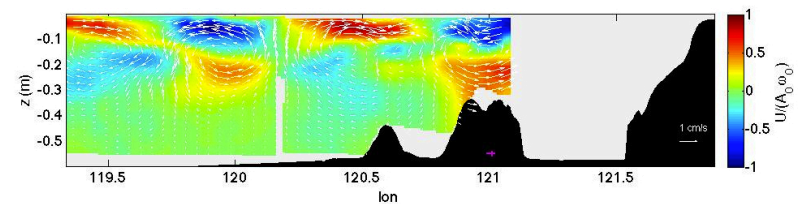
video

K1:

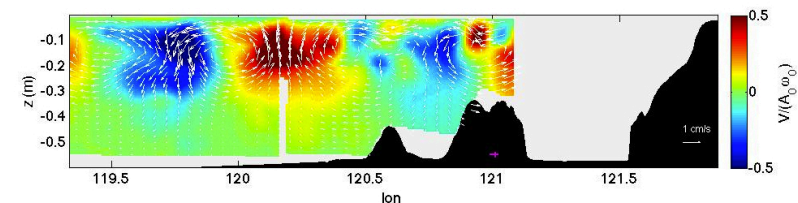


video

*Horizontal velocity:*



*Vertical velocity:*



# The global picture

- Internal tides are generated by significant deep-ocean ridges.

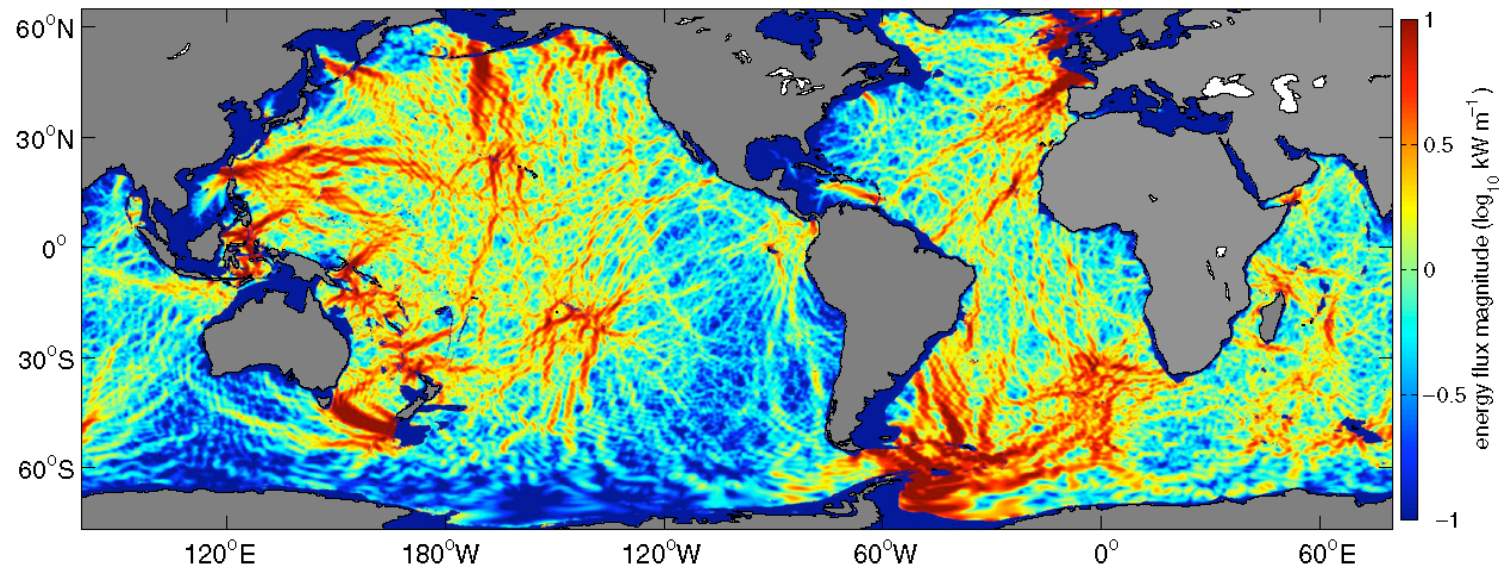


(Image: Simmons 2008)

- The total energy flux in to the deep ocean in the form of internal tides is in the range 0.9-1.2TW.
- There are many other forms of topographic generation process (e.g. lee waves, solitary waves, 3D) but the energy flux from these, while perhaps locally significant, is likely not globally significant (an exception might be the ACC).
- Comparisons between field measurements, theoretical models and numerical simulations all seem to be in accord.

---

**TO BE  
CONTINUED...→**